An algorithmic approach to the multiple impact of a disk in a corner.

An algorithmic approach to the multiple impact of a disk in a corner.*

Claudia Fassino†, Stefano Pasquero‡

Abstract

The paper presents and analyzes the iterative rules determining the impulsive behavior of a rigid disk having a single or possibly multiple frictionless impact with two walls forming a corner.

In the first part, two theoretical iterative rules are presented for the cases of ideal impact and Newtonian frictionless impact with global dissipation index. The termination analysis of the algorithms differentiates the two cases: in the ideal case, it is shown that the algorithm always terminates and the disk exits from the corner after a finite number of steps independently of the initial impact velocity of the disk and the angle formed by the walls; in the non–ideal case, although is not proved that the disk exits from the corner in a finite number of steps, it is shown that its velocity decreases to zero, so that the termination of the algorithm can be fixed through an "almost at rest" condition.

In the second part, it is presented a stable version of both the theoretical algorithms. It is shown that the stable version of the algorithm is more robust than the theoretical ones with respect to noisy initial data and floating point arithmetic computation. The outputs of the stable and theoretical versions of the algorithms are compared, showing that they are similar, even if not coincident, outputs. Moreover, the outputs of the stable version of the algorithm in some meaningful cases are graphically presented and discussed.

The paper clarifies the practical applicability of theoretical methods presented in [Pasquero, 2018] by analyzing the paradigmatic case of the disk in the corner.

2010 Mathematical subject classification: 70E18; 70F35; 70–04
Keywords: Multipoint Impact – Iterative Method

Introduction

The study of the behavior of a rigid or multibody system subject to multiple contact and/or impact is a very actual argument of investigation, finding application in several branches of Classical Mechanics, from the analysis of the motion of billiard balls to that of rocking blocks or granular materials.

The argument can be dealt adopting several different theoretical and/or numerical approaches, and focussing attention on different problems: formalization of the unilateral context, well–posedness of the equations of motion, existence and uniqueness of local or global solutions, energy balance and conservation laws, constitutive characterization of the constraints.

†Department of Mathematics, University of Genova - Via Dodecaneso 35, 16146 GENOVA - email: fassino@dima.unige.it

‡Department of Mathematical, Physical and Computer Sciences, University of Parma. Parco Area delle Scienze 53/a (Campus) 43124 PARMA. email: stefano.pasquero@unipr.it

In a recent paper ([Pasquero, 2018]), a geometric approach framed in the context of jet–bundle theory was used to analyze, starting from a suitable constitutive characterization, the behavior of a general mechanical system with a finite number of degrees of freedom subject to multiple unilateral ideal constraints. Due to the frame invariance requirement that is the rationale of the method, and the requirement of conservation of kinetic energy of the system in the impact, this geometric approach differs in a substantial way from the analytical and numerical methods mostly found in literature, such as the methods based on convex analysis and the LCP methods (see e.g. [Moreau, 1988, Lötstedt, 1982]), the DAE and HHT methods (see e.g. [Haddouni et al., 2017, Negrut et al., 2007]), the differential inclusions and measure derivative methods ([Kiseleva et al., 2018, Monteiro Marques, 1993]), analytical or numerical integration methods ([Moreau, 1999, Paoli and Schatzman, 2002, Liu et al., 2008]. The wide bibliographies of the books of Brogliato ([Brogliato, 2016]) and of Pfeiffer and Glocker ([Pfeiffer and Glocker, 2000]) give a clear idea of the hugeness of the state of the art about these methods. For a survey about the methods, see also [Khulief, 2013, Acary and Brogliato, 2008] and the references therein.

The jet–bundle based geometric method described in [Pasquero, 2018] has its natural applicability in the context of the event–driven analysis of systems subject to frictionless constraints with algebraic–type impact rules, and in this case led to the construction of an iterative rule that, for several significant mechanical systems, determines the theoretical behavior of the system, that is its "right" velocity after the impact, once the "left" velocity of the system before the impact and the geometric and massive properties of the system are known.

In this paper we present the application of this iterative rule to the paradigmatic case of the planar system formed by a rigid disk simultaneously impacting with both sides of a corner in two possible situations: the ideal case, with frictionless contacts and conservation of the kinetic energy of the disk; the so called Newtonian frictionless impact with global dissipation index, a non–ideal case with frictionless contact and no requirement of conservation of kinetic energy.

In the ideal case, the iterative rule for the disk can be directly built starting from the theoretical procedure of [Pasquero, 2018]. Nevertheless, the results presented in this paper for the disk are far from being a pedestrian computation. In addition to the physical meaning of the outputs, the paper is focused on the termination analysis of the algorithm implementing the rule. This is an important aspect of the theoretical approach that was not discussed in [Pasquero, 2018]: although for several meaningful systems the algorithm evidently terminates, it is clear that the requirement of conservation of kinetic energy suggests the possibility of an infinite number of iterations of the algorithm, reflecting the possibility of an infinite number of "rebounds" of the disk on the walls of the corner. We prove that the algorithm applied to the system of the disk always terminates and determines a velocity such that the disk exits from the corner. However, notwithstanding the manifest simplicity of the mechanical system, the analysis lights up two important aspects of multiple ideal impacts: the first is that the geometry of the system, essentially the angle formed by the walls, can be easily arranged in order to obtain as many iterations of the algorithm as one can decide; the second is that the case of effective double impact of the disk with both sides of the corner, although leading to a non trivial non–linear rule for the determination of the right velocity, is however such that that the double impact can happen only once.

The iterative rule for the non–ideal case consists in a generalization of the ideal one supposing that the (frictionless) walls of the corner are partially or totally inelastic. The non–ideality is introduced by a "Newtonian" restitution coefficient ε relating the orthogonal components of the velocity of the disk with respect to the walls before and after each step of the algorithm. Note that, due to the nature of the Newtonian restitution coefficient in the geometric approach, the choice of a totally inelastic coefficient does not implies a sudden stop of the disk ([Fassino and Pasquero, 2019]). Moreover, we recall that, in the geometric approach, Newton's

and Poisson's laws of restitution are equivalent ([Pasquero, 2005]). Although such a modelization was suggested in [Pasquero, 2018] as a natural outgrowth of the ideal case, the details and results of this generalization are, in actual fact, totally new. In this case we do not prove that the algorithm implementing the rule always determines a velocity such that the disk exits from the corner, but we show that the norm of the velocity decreases to 0 for increasing numbers of steps. This gives a second termination criterion for the algorithm, with a meaningful physical interpretation. Moreover we prove that, even in the non–ideal case, double impacts of the disk with both the sides of the corner can happen only once.

However, in case of a pedestrian implementation of the theoretical iterative rules, small perturbations of the input data and approximations of the computed values can cause structural changes in response with consequent different choices in the iterative methods, such as to invalidate the final results (see the example below in Sec. 6). For this reason, we present an algorithm, based on the theoretical rules, that is more robust with respect to the errors due to the measurements and to the use of the floating point arithmetic. This stable version of the algorithm differs from the theoretical rules in the criteria for selecting the behavior of the disk after a rebound. In the theoretical rules such criteria are based on the nullity of some suitable components of the velocity. It is however well known that an exact comparison with zero makes an algorithm unstable, and so, in order to obtain a more robust algorithm, we introduce two thresholds: one determining when a single component of the velocity of the disk is almost zero, one determining when the norm of the whole velocity is almost zero. Furthermore, we compare the theoretical and numerical versions of the algorithms showing that, starting from the same input, they compute the same output in the same number of steps, or they compute slightly different outputs, even if one of the versions performs more steps.

The paper is divided into two main parts: in the first, after some short preliminaries, we introduce the theoretical iterative rule for the ideal impact in three different but equivalent forms and we show the corresponding results. Then we introduce the theoretical algorithm for the non–ideal impact in two different but equivalent forms and we show the corresponding results. In the second part we introduce the stable version of the algorithm that groups both the ideal and the non–ideal theoretical cases. Then we compare the theoretical and numerical versions of the algorithms. Finally, we illustrate the behavior of the stable algorithm by listing the outputs computed processing several different meaningful inputs.

Since the main aim of the paper is focused on the analysis of the algorithms giving the velocity of the disk after the impact, we will limit the mathematical aspects to the bare necessary to describe the rules for the case of the disk in the corner. The Reader interested in a wider description of the geometry and the impulsive aspects of general systems subject to ideal multiple constraints can refer to [Pasquero, 2018] and the references therein. The Reader interested in a short synthesis of the geometric and impulsive theoretical aspects restricted to the case of the disk in the corner can refer to [Fassino and Pasquero, 2019].

The list of possible references about multiple impacts is very huge, and a bibliography claiming to be exhaustive on the argument should be excessively long compared to the length of the paper. Moreover, only few works would be reasonably pertinent to the specific methods used in the paper. Therefore, the list of references has been based on the minimality criterion of making the paper self–consistent. However, for large but not recent or exhaustive lists of general references, see for example [Brogliato, 2016, Johnson, 1985, Stronge, 2000].

PART 1: THEORETICAL ASPECTS

1 Preliminaries

A rigid disk of unitary mass and radius R moves in the part of a horizontal plane delimited by two walls $\mathcal{S}_1, \mathcal{S}_2$ forming an angle $2\alpha \in (0, \pi)$ (see Fig. 1). We can describe the geometry of the system by introducing local coordinates (x, y, ϑ) where x, y are the coordinates of the center of the disk and ϑ is the orientation of the disk. Choosing $k = \tan\alpha$, then $k > 0$ and the walls can be described by the cartesian relations $\mathcal{S}_1 : kx - y = 0$, $\mathcal{S}_2 : kx + y = 0$. Since we adopt the so called *event–driven* approach, we assume that $(x, y) = (-\frac{R}{\sin\alpha}, 0)$ so that the disk is in contact with both the walls. We assume the contacts as frictionless.

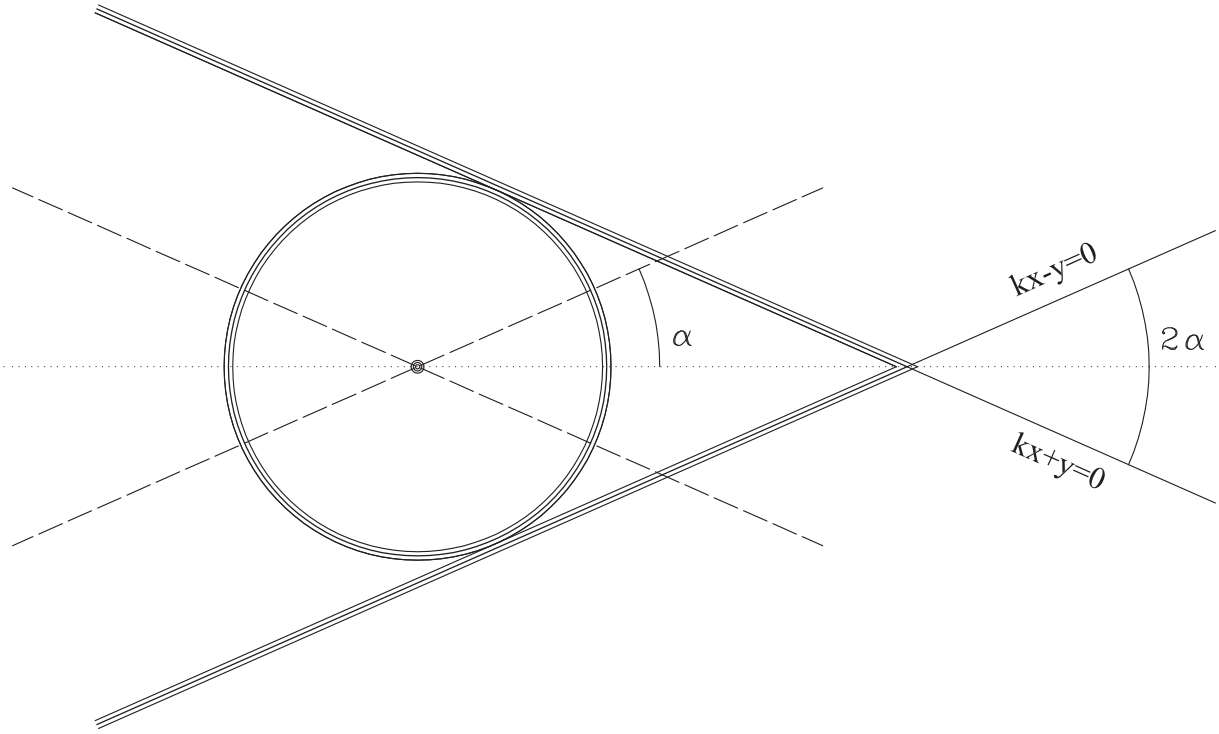

Figure 1: Disk in contact with both sides of the corner

The kinetic state of the disk is known once the linear velocity of the (center of the) disk is assigned through a pair $\mathbf{v} = (\dot{x}, \dot{y})$, and the spin is assigned by $\dot{\vartheta}$. Of course, the linear velocity can be assigned in the alternative form $(v\cos\varphi, v\sin\varphi)$ with $v > 0$ and $\varphi \in (-\pi, \pi]$. Without entering temporarily into mathematical details, it is clear that the angle φ determines the nature of the impact between disk and walls: if $\varphi \in (-\alpha, \alpha)$, the disk is subject to a multiple impact, if $\varphi \in [\alpha, \pi - \alpha)$ the disk is subject to an impact with $\mathcal{S}_2$ and not with $\mathcal{S}_1$, if $\varphi \in (-\pi + \alpha, -\alpha]$ the disk is subject to an impact with $\mathcal{S}_1$ and not with $\mathcal{S}_2$. Otherwise, the velocity $\mathbf{v}$ is a so–called *exit velocity*, the disk does not impact with the walls and its time evolution separates it from one or both the walls.

We can divide the space of the linear velocities of the system into four different zones $\mathcal{Z}_0, \mathcal{Z}_1, \mathcal{Z}_2, \mathcal{Z}_{12}$ with $\mathbf{v} \in \mathcal{Z}_i$ if, with a slight abuse of notation, the linear velocity determines an impact with $\mathcal{S}_i$.

Remark 1. If we restrict our attention to a physically meaningful situation and taking into account Fig. 1, the initial velocity $\mathbf{v}_0 = (\dot{x}_0, \dot{y}_0)$ is such that $\mathbf{v}_0 \in \mathcal{Z}_{12}$ or $\mathbf{v}_0$ is parallel to the walls, that is $\varphi_0 \in [-\alpha, \alpha]$. ♢

We now resume the main consequences of the constitutive characterization of multiple contact/impact presented in [Pasquero, 2018] for the case of the disk in the corner:

0) the constitutive characterization assigns a reactive impulse $\mathbf{I}$ to any kinetic state of the disk supposed in contact with the walls;

1) independently of the kinetic state of the disk, the reactive impulse $\mathbf{I}$ does not involve the spin $\dot{\vartheta}$ of the disk, that remains unchanged in the impact. This is coherent with the assumption that the contacts of the disk with $\mathcal{S}_1$ and $\mathcal{S}_2$ are frictionless. Then we can focus our attention only on the linear part $\mathbf{v}$ of the velocity of the disk;

2) for every linear velocity $\mathbf{v}$ we can determine the orthogonal components $\mathbf{v}_1^{\perp}(\mathbf{v}), \mathbf{v}_2^{\perp}(\mathbf{v})$ of $\mathbf{v}$ with respect to $\mathcal{S}_1, \mathcal{S}_2$ respectively. The orthogonal components indicate if $\mathbf{v}$ is an exit velocity or if $\mathbf{v}$ gives rise to an impact with $\mathcal{S}_1$ and/or $\mathcal{S}_2$. In particular, if $\mathbf{v} = (\dot{x}, \dot{y})$, we have that:

$$
\begin{aligned}
\mathbf{v} \in \mathcal{Z}_0 \quad &\Leftrightarrow \quad \begin{cases} k\dot{x} + \dot{y} \leq 0 \\ k\dot{x} - \dot{y} \leq 0 \end{cases} \\
\mathbf{v} \in \mathcal{Z}_1 \quad &\Leftrightarrow \quad \begin{cases} k\dot{x} + \dot{y} \leq 0 \\ k\dot{x} - \dot{y} > 0 \end{cases} \\
\mathbf{v} \in \mathcal{Z}_2 \quad &\Leftrightarrow \quad \begin{cases} k\dot{x} + \dot{y} > 0 \\ k\dot{x} - \dot{y} \leq 0 \end{cases} \\
\mathbf{v} \in \mathcal{Z}_{12} \quad &\Leftrightarrow \quad \begin{cases} k\dot{x} + \dot{y} > 0 \\ k\dot{x} - \dot{y} > 0 \end{cases}
\end{aligned}
\tag{1}
$$

Note that the symmetry of the mechanical problem is reflected in the symmetry of the zones $\mathcal{Z}_i$ with respect to the $(\dot{x}, \dot{y})$ components of the velocity. In fact we have

$$
\begin{array}{lll}
(\dot{x}_n, \dot{y}_n) \in \mathcal{Z}_0 & \Rightarrow & (\dot{x}_n, -\dot{y}_n) \in \mathcal{Z}_0 \\
(\dot{x}_n, \dot{y}_n) \in \mathcal{Z}_1 & \Rightarrow & (\dot{x}_n, -\dot{y}_n) \in \mathcal{Z}_2 \\
(\dot{x}_n, \dot{y}_n) \in \mathcal{Z}_2 & \Rightarrow & (\dot{x}_n, -\dot{y}_n) \in \mathcal{Z}_1 \\
(\dot{x}_n, \dot{y}_n) \in \mathcal{Z}_{12} & \Rightarrow & (\dot{x}_n, -\dot{y}_n) \in \mathcal{Z}_{12}\,.
\end{array}
$$

3) the constitutive characterization determines a rule assigning a "new" velocity of the system once an "old" velocity is known. The rule is $\mathbf{v}_{new} = \mathbf{v}_{old} + \mathbf{I}(\mathbf{v}_{old})$, where $\mathbf{I}$ represents the reactive impulse generated by the impact with the walls, and the function $\mathbf{I}(\mathbf{v}_{old})$ depends on the ideal or non–ideal nature of the impact.

Of course $\mathbf{I}(\mathbf{v}_{old}) = 0$ if $\mathbf{v} \in \mathcal{Z}_0$: in this case, the reactive impulse acting on the disk is null and the kinetic energy is obviously preserved, as well as the euclidean norm $\|\mathbf{v}\|_2 = \sqrt{\dot{x}^2 + \dot{y}^2}$.

The rule $\mathbf{I} = \mathbf{I}(\mathbf{v}_{old})$ consists in a complete or partial "reflection" of the orthogonal component $\mathbf{v}_i^{\perp}(\mathbf{v}_{old})$ if $\mathbf{v}_{old} \in \mathcal{Z}_i, i = 1, 2$. In the ideal case, the reactive impulse acting on the disk has the form $\mathbf{I}(\mathbf{v}_{old}) = -2\mathbf{v}_i^{\perp}(\mathbf{v}_{old})$, so that the reflection of the component $\mathbf{v}_i^{\perp}(\mathbf{v}_{old})$ is complete. The kinetic energy and $\|\mathbf{v}\|_2$ are once again preserved. In the non–ideal case, the reactive impulse acting on the disk has the form $\mathbf{I}(\mathbf{v}_{old}) = -(1+\varepsilon)\,\mathbf{v}_i^{\perp}(\mathbf{v}_{old})$ with $0 \leq \varepsilon < 1$, so that the reflection of the component $\mathbf{v}_i^{\perp}(\mathbf{v}_{old})$ is only partial. The kinetic energy of the system is not preserved and $\|\mathbf{v}_{new}\|_2 < \|\mathbf{v}_{old}\|_2$.

The rule $\mathbf{I} = \mathbf{I}(\mathbf{v}_{old})$ consists in a strongly non–linear relation in the components of $\mathbf{v}_{old}$ in case of multiple impact $\mathbf{v}_{old} \in \mathcal{Z}_{12}$ (see (3d) and (13d) below): in this case, the reactive impulse has the form $\mathbf{I}(\mathbf{v}_{old}) = \lambda(\mathbf{v}_1^{\perp}(\mathbf{v}_{old}) + \mathbf{v}_2^{\perp}(\mathbf{v}_{old}))$ where λ is a coefficient suitable to obtain the conservation of the kinetic energy in the ideal multiple impact (see [Pasquero, 2018]) or involving the Newtonian restitution coefficient ε in the non–ideal one.

The resulting constitutive characterization can be synthesized with the following assignments, where $\varepsilon \in [0, 1]$ with $\varepsilon = 1$ in the ideal case, and different λ for ideal and non–ideal cases.

$$\begin{array}{lcl} \mathbf{v}_{old} \in \mathcal{Z}_0 & \Rightarrow & \mathbf{v}_{new} = \mathbf{v}_{old} \\ \mathbf{v}_{old} \in \mathcal{Z}_1 & \Rightarrow & \mathbf{v}_{new} = \mathbf{v}_{old} - (1+\varepsilon)\,\mathbf{v}_1^{\perp}(\mathbf{v}_{old}) \\ \mathbf{v}_{old} \in \mathcal{Z}_2 & \Rightarrow & \mathbf{v}_{new} = \mathbf{v}_{old} - (1+\varepsilon)\,\mathbf{v}_2^{\perp}(\mathbf{v}_{old}) \\ \mathbf{v}_{old} \in \mathcal{Z}_{12} & \Rightarrow & \mathbf{v}_{new} = \mathbf{v}_{old} + \lambda\,\left(\mathbf{v}_1^{\perp}(\mathbf{v}_{old}) + \mathbf{v}_2^{\perp}(\mathbf{v}_{old})\right) \end{array} \tag{2}$$

4) the iterative application of the rule determines an algorithm suitable to determine if and how the disk exits from the corner, loosing contact with one or both the walls. The output of the rule become constant if the "new" velocity belongs to the $\mathcal{Z}_0$ zone. Then, both in the ideal and the non–ideal cases, the termination analysis of the algorithm is necessarily related to the condition $\mathbf{v} \in \mathcal{Z}_0$ (or, of course, on the number of steps). In the non–ideal case, the termination analysis can be also based on the condition $\|\mathbf{v}\|_2 \leq \textit{constant}$ upon proof that $\lim_{n\to+\infty} \|\mathbf{v}\|_2 = 0$.

2 Theoretical rule for the ideal case ($\mathbf{TR}_{id}$)

In this section we present the iterative rule assigning the "new" velocity $\mathbf{v}_{n+1}$ of the disk as function of the "old" velocity $\mathbf{v}_n$ for the ideal case in three different forms. Each one of the forms will be used to obtain theoretical results about the algorithm implementing the rule.

2.1 First expression of $\mathbf{TR}_{id}$: use of $(\dot{x}, \dot{y})$

Given an initial velocity $\mathbf{v}_0 = (\dot{x}_0, \dot{y}_0)$, the iterative rule determined by the constitutive characterization of [Pasquero, 2018] is such that:

$$\text{If } (\dot{x}_n, \dot{y}_n) \in \mathcal{Z}_0\,, \quad \text{that is if } \begin{cases} k\dot{x}_n + \dot{y}_n \leq 0 \\ k\dot{x}_n - \dot{y}_n \leq 0 \end{cases}, \quad \text{then } \begin{cases} \dot{x}_{n+1} = \dot{x}_n \\ \dot{y}_{n+1} = \dot{y}_n \end{cases} \tag{3a}$$

$$\text{If } (\dot{x}_n, \dot{y}_n) \in \mathcal{Z}_1\,, \quad \text{that is if } \begin{cases} k\dot{x}_n + \dot{y}_n \leq 0 \\ k\dot{x}_n - \dot{y}_n > 0 \end{cases}, \quad \text{then } \begin{cases} \dot{x}_{n+1} = \dfrac{1-k^2}{1+k^2}\,\dot{x}_n + \dfrac{2k}{1+k^2}\,\dot{y}_n \\ \dot{y}_{n+1} = \dfrac{2k}{1+k^2}\,\dot{x}_n - \dfrac{1-k^2}{1+k^2}\,\dot{y}_n \end{cases} \tag{3b}$$

$$\text{If } (\dot{x}_n, \dot{y}_n) \in \mathcal{Z}_2\,, \quad \text{that is if } \begin{cases} k\dot{x}_n + \dot{y}_n > 0 \\ k\dot{x}_n - \dot{y}_n \leq 0 \end{cases}, \quad \text{then } \begin{cases} \dot{x}_{n+1} = \dfrac{1-k^2}{1+k^2}\,\dot{x}_n - \dfrac{2k}{1+k^2}\,\dot{y}_n \\ \dot{y}_{n+1} = -\dfrac{2k}{1+k^2}\,\dot{x}_n - \dfrac{1-k^2}{1+k^2}\,\dot{y}_n \end{cases} \tag{3c}$$

$$\text{If } (\dot{x}_n, \dot{y}_n) \in \mathcal{Z}_{12}\,, \quad \text{that is if } \begin{cases} k\dot{x}_n + \dot{y}_n > 0 \\ k\dot{x}_n - \dot{y}_n > 0 \end{cases}, \quad \text{then } \begin{cases} \dot{x}_{n+1} = \dfrac{-k^4\dot{x}_n^2 + (1-2k^2)\dot{y}_n^2}{k^4\dot{x}_n^2 + \dot{y}_n^2}\,\dot{x}_n \\ \dot{y}_{n+1} = \dfrac{k^2(k^2-2)\dot{x}_n^2 - \dot{y}_n^2}{k^4\dot{x}_n^2 + \dot{y}_n^2}\,\dot{y}_n \end{cases} \tag{3d}$$

REMARK 2. A straightforward calculation shows that independently of the condition $\mathbf{v}_n \in \mathcal{Z}_i$ with $i = 0, 1, 2, 12$, we have

$$\frac{(\|\mathbf{v}_{n+1}\|_2)^2}{(\|\mathbf{v}_n\|_2)^2} = \frac{\dot{x}_{n+1}^2 + \dot{y}_{n+1}^2}{\dot{x}_n^2 + \dot{y}_n^2} = 1\,. \tag{4}$$

This is an easily predictable but not trivial consequence of the preservation of the kinetic energy required in [Pasquero, 2018]. In fact, since the kinetic energy is not an absolute quantity but it depends on the choice of a frame of reference, the validity of (4) follows from the nature itself of the contact/impact, that does not affect the angular coordinate of the disk, and the nature itself of the constraint and its set of rest frames. Moreover, $\|\mathbf{v}\|_2$ is not the norm of the velocity vector of the disk but only the Euclidean norm of the pair $(\dot{x}, \dot{y})$ viewed as an element of $\mathbb{R}^2$ (see the Appendix of [Fassino and Pasquero, 2019] for details). ♢

REMARK 3. The rule (3a–3d) respects the symmetry of the mechanical problem with respect to the $(\dot{x}, \dot{y})$ components of the velocity. In fact an easy calculation shows that, if $(\dot{x}_n, \dot{y}_n) \notin \mathcal{Z}_0$, then

$$\left\{ \begin{array}{rcl} \dot{x}_{n+1}(\dot{x}_n, -\dot{y}_n) & = & \dot{x}_{n+1}(\dot{x}_n, \dot{y}_n) \\ \dot{y}_{n+1}(\dot{x}_n, -\dot{y}_n) & = & -\dot{y}_{n+1}(\dot{x}_n, \dot{y}_n) \end{array} \right. \tag{5}$$

♢

2.2 Second expression of TR_{id}: use of $(\cos\varphi, \sin\varphi)$

The rule (3a–3d) can be expressed using $\mathbf{v}_0$ in the form $(v_0 \cos\varphi_0, v_0 \sin\varphi_0)$ with $v_0 > 0$, $\varphi \in (\pi, \pi]$. Since $k = \tan\alpha$ so that

$$\left\{ \begin{array}{rcl} \dfrac{1-k^2}{1+k^2} & = & \cos 2\alpha \\[2ex] \dfrac{2k}{1+k^2} & = & \sin 2\alpha\,, \end{array} \right.$$

we immediately obtain that the matrices of the linear transformations given by (3b,3c) are orthogonal but not special orthogonal. Moreover, thanks to (4), v_0 is factorized in every term. The rule becomes

$$\text{If } \mathbf{v}_n \in \mathcal{Z}_0\,, \quad \text{that is if} \quad \left\{ \begin{array}{l} \cos\varphi_n < 0 \\ |\tan\varphi_n| \le \tan\alpha \end{array} \right. , \quad \text{then} \quad \varphi_{n+1} = \varphi_n \tag{6a}$$

$$\text{If } \mathbf{v}_n \in \mathcal{Z}_1\,, \quad \text{that is if} \quad \left\{ \begin{array}{l} \sin\varphi_n < 0 \\ -\cot\alpha < \cot\varphi_n \le \cot\alpha \end{array} \right. , \quad \text{then} \quad \varphi_{n+1} = -\varphi_n + 2\alpha \tag{6b}$$

$$\text{If } \mathbf{v}_n \in \mathcal{Z}_2\,, \quad \text{that is if} \quad \left\{ \begin{array}{l} \sin\varphi_n > 0 \\ -\cot\alpha < \cot\varphi_n \le \cot\alpha \end{array} \right. , \quad \text{then} \quad \varphi_{n+1} = -\varphi_n - 2\alpha \tag{6c}$$

$$\text{If } \mathbf{v}_n \in \mathcal{Z}_{12}, \quad \text{that is if} \quad \left\{ \begin{array}{l} \cos\varphi_n > 0 \\ |\tan\varphi_n| < \tan\alpha \end{array} \right. , \quad \text{then}$$

$$\left\{ \begin{array}{rcl} \cos\varphi_{n+1} & = & -\left(\dfrac{\tan^4\alpha\cos^2\varphi_n - \sin^2\varphi_n}{\tan^4\alpha\cos^2\varphi_n + \sin^2\varphi_n} + 2\,\dfrac{\tan^2\alpha\sin^2\varphi_n}{\tan^4\alpha\cos^2\varphi_n + \sin^2\varphi_n} \right) \cos\varphi_n \\[2ex] \sin\varphi_{n+1} & = & \left(\dfrac{\tan^4\alpha\cos^2\varphi_n - \sin^2\varphi_n}{\tan^4\alpha\cos^2\varphi_n + \sin^2\varphi_n} - 2\,\dfrac{\tan^2\alpha\cos^2\varphi_n}{\tan^4\alpha\cos^2\varphi_n + \sin^2\varphi_n} \right) \sin\varphi_n \end{array} \right. \tag{6d}$$

2.3 Third expression of TR$_{id}$: use of $(\dot\xi, \dot\eta)$

A third version of the rule (3a–3d) can be obtained by using a standard change of coordinates $(\xi, \eta) = (kx + y, kx - y)$ that identifies the velocity using its projections in the directions of the walls. Then we have

$$\left\{ \begin{array}{l} \dot\xi \,=\, k\dot x + \dot y \\ \dot\eta \,=\, k\dot x - \dot y \end{array} \right. \quad \Leftrightarrow \quad \left\{ \begin{array}{l} \dot x \,=\, \dfrac{\dot\xi + \dot\eta}{2k} \\ \\ \dot y \,=\, \dfrac{\dot\xi - \dot\eta}{2} \end{array} \right. . \tag{7}$$

In this case we have:

$$\text{If } (\dot\xi_n, \dot\eta_n) \in \mathcal{Z}_0\,, \quad \text{that is if} \quad \left\{ \begin{array}{l} \dot\xi_n \le 0 \\ \dot\eta_n \le 0 \end{array} \right. , \quad \text{then} \quad \left\{ \begin{array}{l} \dot\xi_{n+1} \,=\, \dot\xi_n \\ \dot\eta_{n+1} \,=\, \dot\eta_n \end{array} \right. \tag{8a}$$

$$\text{If } (\dot\xi_n, \dot\eta_n) \in \mathcal{Z}_1\,, \quad \text{that is if} \quad \left\{ \begin{array}{l} \dot\xi_n \le 0 \\ \dot\eta_n > 0 \end{array} \right. , \quad \text{then} \quad \left\{ \begin{array}{l} \dot\xi_{n+1} \,=\, \dot\xi_n \,+\, 2\,\dfrac{1-k^2}{1+k^2}\,\dot\eta_n \\ \\ \dot\eta_{n+1} \,=\, -\,\dot\eta_n \end{array} \right. \tag{8b}$$

$$\text{If } (\dot\xi_n, \dot\eta_n) \in \mathcal{Z}_2\,, \quad \text{that is if} \quad \left\{ \begin{array}{l} \dot\xi_n > 0 \\ \dot\eta_n \le 0 \end{array} \right. , \quad \text{then} \quad \left\{ \begin{array}{l} \dot\xi_{n+1} \,=\, -\,\dot\xi_n \\ \\ \dot\eta_{n+1} \,=\, \dot\eta_n \,+\, 2\,\dfrac{1-k^2}{1+k^2}\,\dot\xi_n \end{array} \right. \tag{8c}$$

$$\text{If } (\dot\xi_n, \dot\eta_n) \in \mathcal{Z}_{12}\,, \quad \text{that is if} \quad \left\{ \begin{array}{l} \dot\xi_n > 0 \\ \dot\eta_n > 0 \end{array} \right. , \quad \text{then} \quad \left\{ \begin{array}{rcl} \dot\xi_{n+1} & = & -\,\dfrac{(1+k^2)(\dot\xi_n^2 + \dot\eta_n^2) + 2(1-k^2)\dot\xi_n\dot\eta_n}{(1+k^2)(\dot\xi_n^2 + \dot\eta_n^2) - 2(1-k^2)\dot\xi_n\dot\eta_n}\,\dot\xi_n \\ \\ & & +\,2\,\dfrac{(1-k^2)(\dot\xi_n^2 + \dot\eta_n^2)}{(1+k^2)(\dot\xi_n^2 + \dot\eta_n^2) - 2(1-k^2)\dot\xi_n\dot\eta_n}\,\dot\eta_n \\ \\ \dot\eta_{n+1} & = & 2\,\dfrac{(1-k^2)(\dot\xi_n^2 + \dot\eta_n^2)}{(1+k^2)(\dot\xi_n^2 + \dot\eta_n^2) - 2(1-k^2)\dot\xi_n\dot\eta_n}\,\dot\xi_n \\ \\ & & -\,\dfrac{(1+k^2)(\dot\xi_n^2 + \dot\eta_n^2) + 2(1-k^2)\dot\xi_n\dot\eta_n}{(1+k^2)(\dot\xi_n^2 + \dot\eta_n^2) - 2(1-k^2)\dot\xi_n\dot\eta_n}\,\dot\eta_n \end{array} \right. \tag{8d}$$

Remark 4. Note that, due to the change of coordinates (7), we have:

$$(\|\mathbf{v}_n\|_2)^2 \,=\, \frac{1+k^2}{4k^2}\left(\dot\xi_n^2 + \dot\eta_n^2\right) + \frac{1-k^2}{2k^2}\,\dot\xi_n\dot\eta_n$$

$\Diamond$

3 Theoretical results about TR$_{id}$

Several results and some remarks can be listed about TR$_{id}$. Some of them can be straightforwardly obtained by one or more of the expressions of the algorithm, some others requires a detailed proof.

RESULT 1. If $\mathbf{v}_n \in \mathcal{Z}_1$ then $\mathbf{v}_{n+1} \in \mathcal{Z}_2$ or $\mathbf{v}_{n+1} \in \mathcal{Z}_0$. Analogously, if $\mathbf{v}_n \in \mathcal{Z}_2$ then $\mathbf{v}_{n+1} \in \mathcal{Z}_1$ or $\mathbf{v}_{n+1} \in \mathcal{Z}_0$.

PROOF: It follows immediately from (8b,8c). If $\mathbf{v}_n \in \mathcal{Z}_1$ then $\eta_n > 0$. Then $\eta_{n+1} = -\eta_n < 0$, so that $\mathbf{v}_{n+1} \in \mathcal{Z}_2$ or $\mathbf{v}_{n+1} \in \mathcal{Z}_0$. The proof is analogous if $\mathbf{v}_n \in \mathcal{Z}_2$. □

This shows that, if an iteration of TR_{id} gives a velocity $\mathbf{v} \notin \mathcal{Z}_{12}$, then all the following velocities do not belong to $\mathcal{Z}_{12}$. In particular, if $\mathbf{v}_0 \notin \mathcal{Z}_{12}$, than the evolution of the disk will be determined by a sequence of single impacts, without multiple impacts.

RESULT 2. If $\mathbf{v}_n \in \mathcal{Z}_1$ and $k \geq 1$ then $\mathbf{v}_{n+1} \in \mathcal{Z}_0$. Analogously, if $\mathbf{v}_n \in \mathcal{Z}_2$ and $k \geq 1$ then $\mathbf{v}_{n+1} \in \mathcal{Z}_0$.

PROOF: It follows once again from (8b,8c). If $\mathbf{v}_n \in \mathcal{Z}_1$ then $\xi_n \leq 0$ and $\eta_n > 0$. Therefore, if $k \geq 1$, we have $\xi_{n+1} = \xi_n + 2\dfrac{1-k^2}{1+k^2}\eta_n < 0$, so that $\mathbf{v}_{n+1} \in \mathcal{Z}_0$. The proof is analogous if $\mathbf{v}_n \in \mathcal{Z}_2$. □

This shows that if the angle $2\alpha \geq \frac{\pi}{2}$ and the impact is not multiple we have only one iteration of TR_{id}. This is the case, for instance, when $2\alpha \geq \frac{\pi}{2}$, the disk moves along one of the wall and impacts the other wall.

RESULT 3. If $\mathbf{v}_n \in \mathcal{Z}_1$ then there exists $\chi \in \mathbb{N}$ such that $\mathbf{v}_{n+\chi} \in \mathcal{Z}_0$. Analogously, if $\mathbf{v}_n \in \mathcal{Z}_2$ then there exists $\chi \in \mathbb{N}$ such that $\mathbf{v}_{n+\chi} \in \mathcal{Z}_0$.

PROOF: This is a standard proof about reflections following from (6b,6c). If $\mathbf{v}_n \in \mathcal{Z}_1$ or $\mathcal{Z}_2$ and $k \geq 1$ the thesis follows from the point 2) above.

If $\mathbf{v}_n \in \mathcal{Z}_1$ and $k < 1$, then $\alpha \in (0, \frac{\pi}{4})$ and $\varphi_n \in (-\pi + \alpha, -\alpha]$. We can construct the odd and even subsequences of the sequence φ_{n+r} with $r \in \mathbb{N}$. We have that:

$$\begin{cases} \varphi_{n+2r} &= \varphi_n - 2(2r)\alpha \\ \varphi_{n+2r+1} &= -\varphi_n + 2(2r+1)\alpha \end{cases}.$$

Then χ is the first natural number such that

$$\varphi_n - 2(2\chi)\alpha \quad \text{or} \quad -\varphi_n + 2(2\chi+1)\alpha \in (-\pi, -\pi+\alpha] \cup [\pi-\alpha, \pi]. \tag{9}$$

The proof is analogous if $\mathbf{v}_n \in \mathcal{Z}_2$. □

This shows that, if an iteration of TR_{id} gives a velocity $\mathbf{v} \notin \mathcal{Z}_{12}$, then TR_{id} terminates, giving a final exit velocity for the disk. Note moreover that the reflection procedure of this situation is conceptually identical to the well known one governing the (alternated) single impacts of a disk with the walls of a corner in a sequence of configurations of single (and not multiple) contacts between disk and walls.

The three results above pertain TR_{id} applied in the case of single impact of the disk in the corner. However the most significant results are those about multiple impacts. Note that the condition $\mathbf{v}_n \in \mathcal{Z}_{12}$ implies that $\dot{x}_n > 0$ and $\cos\varphi_n > 0$. We have that:

RESULT 4. If $\mathbf{v}_n \in \mathcal{Z}_{12}$ has the direction of the angle bisector, then $\mathbf{v}_{n+1} = -\mathbf{v}_n \in \mathcal{Z}_0$.

PROOF: It follows immediately from (3d) requiring $\dot{y}_n = 0$ or alternatively from (6d) requiring $\cos\varphi_n = 1, \sin\varphi_n = 0$. □

The main result about multiple impacts is however the following:

Theorem 3.1 *If* $\mathbf{v}_n \in \mathcal{Z}_{12}$ *then* $\mathbf{v}_{n+1} \notin \mathcal{Z}_{12}$.

PROOF: Let $\mathbf{v}_n \in \mathcal{Z}_{12}$ and let us consider (8d). Then $\dot{\xi}_n > 0, \dot{\eta}_n > 0$. If $\dot{\xi}_n = \dot{\eta}_n$ then $\mathbf{v}_n$ has the direction of the angle bisector and we have the thesis. Otherwise, setting for brevity $\rho_n = \dfrac{2\xi_n\eta_n}{\dot{\xi}_n^2 + \dot{\eta}_n^2}, \rho_n \in (0,1)$, a straightforward calculation (see [Fassino and Pasquero, 2019] for details) shows that

$$\begin{cases} \dot{\xi}_{n+1} &= \dfrac{\dot{\xi}_n}{(1+k^2) - \rho_n(1-k^2)} \left(-(1+k^2) - \rho_n(1-k^2) + 2\,\dfrac{\dot{\eta}_n}{\dot{\xi}_n}(1-k^2) \right) \\ \dot{\eta}_{n+1} &= \dfrac{\dot{\eta}_n}{(1+k^2) - \rho_n(1-k^2)} \left(-(1+k^2) - \rho_n(1-k^2) + 2\,\dfrac{\dot{\xi}_n}{\dot{\eta}_n}(1-k^2) \right) \end{cases} \tag{10}$$

Suppose by contradiction that $\mathbf{v}_{n+1} \in \mathcal{Z}_{12}$: then we must have $\dot{\xi}_{n+1} > 0, \dot{\eta}_{n+1} > 0$, that recalling the expression of ρ_n, implies

$$\begin{cases} 2\,(1-k^2)\dfrac{\dot{\eta}_n}{\dot{\xi}_n}\,\dfrac{\dot{\eta}_n^2}{\dot{\xi}_n^2 + \dot{\eta}_n^2} &> (1+k^2) \\ 2\,(1-k^2)\dfrac{\dot{\xi}_n}{\dot{\eta}_n}\,\dfrac{\dot{\xi}_n^2}{\dot{\xi}_n^2 + \dot{\eta}_n^2} &> (1+k^2) \end{cases} \tag{11}$$

This is possible only if $1-k^2 > 0$, so that let $k \in (0,1)$. Since the function $f(k) = \dfrac{1+k^2}{2(1-k^2)} > \dfrac{1}{2}$ if $k \in (0,1)$, then a necessary condition for $\mathbf{v}_{n+1} \in \mathcal{Z}_{12}$ is:

$$\begin{cases} \dfrac{\dot{\eta}_n}{\dot{\xi}_n}\,\dfrac{1}{\dfrac{\dot{\xi}_n^2 + \dot{\eta}_n^2}{\dot{\eta}_n^2}} &> \dfrac{1}{2} \\ \dfrac{\dot{\xi}_n}{\dot{\eta}_n}\,\dfrac{1}{\dfrac{\dot{\xi}_n^2 + \dot{\eta}_n^2}{\dot{\xi}_n^2}} &> \dfrac{1}{2} \end{cases} \tag{12}$$

that has no solutions in $\frac{\dot{\eta}_n}{\dot{\xi}_n} > 0$. Then $\mathbf{v}_{n+1} \notin \mathcal{Z}_{12}$. □

We have then the following:

Corollary 3.1 *For every initial velocity* $\mathbf{v}_0$ *of the disk, the algorithm terminates after a finite number of steps.*

PROOF: If $\mathbf{v}_0 \in \mathcal{Z}_0$, there is nothing to proof. If $\mathbf{v}_0 \in \mathcal{Z}_1$ or $\mathbf{v}_0 \in \mathcal{Z}_2$, the thesis follows from Result 3 of this section. If $\mathbf{v}_0 \in \mathcal{Z}_{12}$, then $\mathbf{v}_1 \notin \mathcal{Z}_{12}$ and then we have the thesis. □

RESULT 5. Theorem 3.1 and Result 1 imply that the system can have at most one multiple impact if and only if $\mathbf{v}_0 \in \mathcal{Z}_{12}$.

RESULT 6. If $\mathbf{v}_0 \in \mathcal{Z}_1$, condition (9) with $\varphi_n = \varphi_0$ gives the number of iterations of the algorithm. An analogous condition holds if $\mathbf{v}_0 \in \mathcal{Z}_2$. If $\mathbf{v}_0 \in \mathcal{Z}_{12}$, the number of iterations is given by condition (9) with $\varphi_n = \varphi_1$ increased by 1.

4 Theoretical rule for the non–ideal case (TR_{nid})

In this section we present two different forms of the rule assigning the "new" velocity $\mathbf{v}_{n+1}$ of the disk as function of the "old" velocity $\mathbf{v}_n$ in the non–ideal case. They are generalizations to non–ideal impacts (see [Fassino and Pasquero, 2019]) of the characterization of ideal impacts. Each one of the forms will be used to obtain theoretical results about TR_{nid}.

4.1 First expression of TR_{nid}: use of $(\dot{x}, \dot{y})$

Given an initial velocity $\mathbf{v}_0 = (\dot{x}_0, \dot{y}_0)$, the rule is such that:

$$\text{If } (\dot{x}_n, \dot{y}_n) \in \mathcal{Z}_0\,, \quad \text{that is if } \begin{cases} k\dot{x}_n + \dot{y}_n \le 0 \\ k\dot{x}_n - \dot{y}_n \le 0 \end{cases}, \quad \text{then } \begin{cases} \dot{x}_{n+1} = \dot{x}_n \\ \dot{y}_{n+1} = \dot{y}_n \end{cases} \tag{13a}$$

$$\text{If } (\dot{x}_n, \dot{y}_n) \in \mathcal{Z}_1\,, \quad \text{that is if } \begin{cases} k\dot{x}_n + \dot{y}_n \le 0 \\ k\dot{x}_n - \dot{y}_n > 0 \end{cases}, \quad \text{then } \begin{cases} \dot{x}_{n+1} = \dfrac{1-\varepsilon k^2}{1+k^2}\,\dot{x}_n + \dfrac{(1+\varepsilon)k}{1+k^2}\,\dot{y}_n \\ \dot{y}_{n+1} = \dfrac{(1+\varepsilon)k}{1+k^2}\,\dot{x}_n - \dfrac{\varepsilon-k^2}{1+k^2}\,\dot{y}_n \end{cases} \tag{13b}$$

$$\text{If } (\dot{x}_n, \dot{y}_n) \in \mathcal{Z}_2\,, \quad \text{that is if } \begin{cases} k\dot{x}_n + \dot{y}_n > 0 \\ k\dot{x}_n - \dot{y}_n \le 0 \end{cases}, \quad \text{then } \begin{cases} \dot{x}_{n+1} = \dfrac{1-\varepsilon k^2}{1+k^2}\,\dot{x}_n - \dfrac{(1+\varepsilon)k}{1+k^2}\,\dot{y}_n \\ \dot{y}_{n+1} = -\dfrac{(1+\varepsilon)k}{1+k^2}\,\dot{x}_n - \dfrac{\varepsilon-k^2}{1+k^2}\,\dot{y}_n \end{cases} \tag{13c}$$

$$\text{If } (\dot{x}_n, \dot{y}_n) \in \mathcal{Z}_{12}\,, \quad \text{that is if } \begin{cases} k\dot{x}_n + \dot{y}_n > 0 \\ k\dot{x}_n - \dot{y}_n > 0 \end{cases}, \quad \text{then } \begin{cases} \dot{x}_{n+1} = \dfrac{-\varepsilon k^4\dot{x}_n^2 + (1-(1+\varepsilon)k^2)\dot{y}_n^2}{k^4\dot{x}_n^2 + \dot{y}_n^2}\,\dot{x}_n \\ \dot{y}_{n+1} = \dfrac{k^2(k^2-(1+\varepsilon))\dot{x}_n^2 - \varepsilon\dot{y}_n^2}{k^4\dot{x}_n^2 + \dot{y}_n^2}\,\dot{y}_n \end{cases} \tag{13d}$$

Remark 5. The rule (13a–13d) once again respects the symmetry of the mechanical problem with respect to the $(\dot{x}, \dot{y})$ components of the velocity, since relations (5) hold for every $\mathbf{v}_n \notin \mathcal{Z}_0$. ◊

4.2 Second expression of TR_{nid}: use of $(\dot{\xi}, \dot{\eta})$

The rule (13a–13d) can be expressed once again by using the coordinates $(\xi, \eta) = (kx+y, kx-y)$. We obtain:

$$\text{If } (\dot{\xi}_n, \dot{\eta}_n) \in \mathcal{Z}_0, \quad \text{that is if } \begin{cases} \dot{\xi}_n \le 0 \\ \dot{\eta}_n \le 0 \end{cases}, \quad \text{then } \begin{cases} \dot{\xi}_{n+1} = \dot{\xi}_n \\ \dot{\eta}_{n+1} = \dot{\eta}_n \end{cases} \tag{14a}$$

$$\text{If } (\dot{\xi}_n, \dot{\eta}_n) \in \mathcal{Z}_1, \quad \text{that is if } \begin{cases} \dot{\xi}_n \le 0 \\ \dot{\eta}_n > 0 \end{cases}, \quad \text{then } \begin{cases} \dot{\xi}_{n+1} = \dot{\xi}_n + (1+\varepsilon)\dfrac{1-k^2}{1+k^2}\dot{\eta}_n \\ \dot{\eta}_{n+1} = -\varepsilon\dot{\eta}_n \end{cases} \tag{14b}$$

$$\text{If } (\dot\xi_n,\dot\eta_n)\in\mathcal{Z}_2,\quad \text{that is if}\quad \left\{\begin{array}{l}\dot\xi_n>0\\ \dot\eta_n\le 0\end{array}\right.,\quad \text{then}\quad \left\{\begin{array}{l}\dot\xi_{n+1}\;=\;-\varepsilon\dot\xi_n\\ \\ \dot\eta_{n+1}\;=\;\dot\eta_n+(1+\varepsilon)\dfrac{1-k^2}{1+k^2}\dot\xi_n\end{array}\right. \tag{14c}$$

$$\text{If } (\dot\xi_n,\dot\eta_n)\in\mathcal{Z}_{12},\quad \text{that is if}\quad \left\{\begin{array}{l}\dot\xi_n>0\\ \dot\eta_n>0\end{array}\right.,\quad \text{then}\quad \left\{\begin{array}{rcl}\dot\xi_{n+1} &=& -\dfrac{\varepsilon(1+k^2)(\dot\xi_n^2+\dot\eta_n^2)+2(1-k^2)\dot\xi_n\dot\eta_n}{(1+k^2)(\dot\xi_n^2+\dot\eta_n^2)-2(1-k^2)\dot\xi_n\dot\eta_n}\dot\xi_n\\ \\ && +(1+\varepsilon)\dfrac{(1-k^2)(\dot\xi_n^2+\dot\eta_n^2)}{(1+k^2)(\dot\xi_n^2+\dot\eta_n^2)-2(1-k^2)\dot\xi_n\dot\eta_n}\dot\eta_n\\ \\ \dot\eta_{n+1} &=& (1+\varepsilon)\dfrac{(1-k^2)(\dot\xi_n^2+\dot\eta_n^2)}{(1+k^2)(\dot\xi_n^2+\dot\eta_n^2)-2(1-k^2)\dot\xi_n\dot\eta_n}\dot\xi_n\\ \\ && -\dfrac{\varepsilon(1+k^2)(\dot\xi_n^2+\dot\eta_n^2)+2(1-k^2)\dot\xi_n\dot\eta_n}{(1+k^2)(\dot\xi_n^2+\dot\eta_n^2)-2(1-k^2)\dot\xi_n\dot\eta_n}\dot\eta_n\end{array}\right. \tag{14d}$$

5 Theoretical results about TR_{nid}

Several results and some remarks that can be listed about TR_{nid} are strictly analogous to those about TR_{id}. For instance, Results 1, 2 and 4 can be immediately generalized to the non–ideal case, with proofs and remarks analogous to those presented in Sec.3. Theorem 3.1 too holds in the non–ideal case, as we prove below in this section. Instead, in the non–ideal case we cannot state the analogous of Result 3 of Sec.3, that in the ideal case is crucial to prove that TR_{id} terminates. However, for TR_{nid}, the termination will be ensured on the basis of the criterion $\lim_{n\to+\infty}\|\mathbf{v}_n\|_2=0$ of the following Theorem 5.3.

Theorem 5.1 *If* $\mathbf{v}_n\in\mathcal{Z}_{12}$ *then* $\mathbf{v}_{n+1}\notin\mathcal{Z}_{12}$.

Proof: Let $\mathbf{v}_n$ be in $\mathcal{Z}_{12}$, so that $\dot\xi_n>0$ and $\dot\eta_n>0$. Recalling that $\varepsilon\in[0,1)$ and $k\in(0,+\infty)$, we set

$$\beta\;=\;\frac{1-k^2}{1+k^2}\;\in(-1,1),\qquad z\;=\;\frac{\dot\eta_n}{\dot\xi_n}\;\in(0,+\infty)\,.$$

Eqs. (14d) can be rewritten as

$$\left\{\begin{array}{rcl}\dot\xi_{n+1} &=& \dfrac{\dot\xi_n}{1-\beta\dfrac{2z}{1+z^2}}\left(-\varepsilon+\beta\left((1+\varepsilon)z-\dfrac{2z}{1+z^2}\right)\right)\\ \\ \dot\eta_{n+1} &=& \dfrac{\dot\eta_n}{1-\beta\dfrac{2z}{1+z^2}}\left(-\varepsilon+\beta\left((1+\varepsilon)\dfrac{1}{z}-\dfrac{2z}{1+z^2}\right)\right)\end{array}\right.$$

where the two first factors of the RHSs are positive. Then $\mathbf{v}_{n+1}\notin\mathcal{Z}_{12}$ if and only if the system of inequalities

$$\left\{\begin{array}{l}-\varepsilon+\beta\left((1+\varepsilon)z-\dfrac{2z}{1+z^2}\right)\;>\;0\\ \\ -\varepsilon+\beta\left((1+\varepsilon)\dfrac{1}{z}-\dfrac{2z}{1+z^2}\right)\;>\;0\end{array}\right. \tag{15}$$

does not admit solutions for $\varepsilon \in [0,1), \beta \in (-1,1), z \in (0,+\infty)$. Obviously (15) does not have solutions if $\beta = 0$ (that is when the amplitude 2α of the corner is $\frac{\pi}{2}$), if $z = 1$ (that is when $\mathbf{v}_n$ is along the bisector of the corner), if $(1+\varepsilon)z - \frac{2z}{1+z^2} = 0$, if $(1+\varepsilon)\frac{1}{z} - \frac{2z}{1+z^2} = 0$.

If $\varepsilon = 0, \beta \in (-1,0) \cup (0,1)$, straightforward calculation show that (15) has no solutions $z \in (0,+\infty)$.

If $\varepsilon \in (0,1), \beta \in (0,1), z \in (0,1)$, then the first inequality of (15) can be verified only if $(1+\varepsilon)z - \frac{2z}{1+z^2} > 0$. In this case we have:

$$\beta > \frac{\varepsilon}{(1+\varepsilon)z - \dfrac{2z}{1+z^2}} = \frac{\varepsilon(1+z^2)}{(1+\varepsilon)(z+z^3) - 2z}$$

This can happen only if

$$\frac{\varepsilon(1+z^2)}{(1+\varepsilon)(z+z^3) - 2z} < 1 \qquad \Leftrightarrow \qquad \varepsilon < -\frac{z(1+z)}{1+z^2} < 0$$

that is not admissible. If $\varepsilon \in (0,1), \beta \in (0,1), z \in (1,+\infty)$, then the second inequality of (15) can be verified only if $(1+\varepsilon)\frac{1}{z} - \frac{2z}{1+z^2} > 0$. In this case we have:

$$\beta > \frac{\varepsilon}{(1+\varepsilon)\frac{1}{z} - \dfrac{2z}{1+z^2}} = \frac{\varepsilon\, z(1+z^2)}{(1+\varepsilon)(1+z^2) - 2z^2}$$

This can happen only if

$$\frac{\varepsilon\, z(1+z^2)}{(1+\varepsilon)(1+z^2) - 2z^2} < 1 \qquad \Leftrightarrow \qquad \varepsilon < -\frac{1+z}{1+z^2} < 0$$

that is not admissible. It follows that (15) cannot have solutions, and then $\mathbf{v}_{n+1} \notin \mathcal{Z}_{12}$. □

RESULT 7. Theorem 5.1 and Result 1 (that holds for non–ideal impacts too) imply once again that the system can have at most one multiple impact if and only if $\mathbf{v}_0 \in \mathcal{Z}_{12}$.

To proof the second important result about TR_{nid} we need to introduce the convergent matrices and their properties. Let A be an $N \times N$ matrix and let $\rho(A)$ its spectral radius, that is the largest modulus of its eigenvalues. We recall that the matrix A is said to be convergent if $\lim_{k\to+\infty}(A^k)_{ij} = 0$ for each $i,j = 1,\ldots,N$, where $(A^k)_{ij}$ is the (i,j)-th element of A^k. The following theorem (see e.g. Theorem 4 in [Isaacson and Keller, 1994, p. 14]) shows some well-known properties of a convergent matrix.

Theorem 5.2 *The following three statements are equivalent:*

1. *the matrix A is convergent;*
2. $\lim_{k\to+\infty} \|A^k\| = 0$ *for some matrix norm induced by a vector norm, that is defined by* $\|A\| = \max_{\|x\|=1} \|Ax\|$*;*
3. $\rho(A) < 1$.

REMARK 6. Let A be a convergent matrix and let $\|\cdot\|$ be the induced matrix norm for which item 2 of Theorem 5.2 holds. Given a vector $\mathbf{w}$, we have, from a property of the induced matrix norm, that $0 \le \|A^k\mathbf{w}\| \le \|A^k\|\|\mathbf{w}\|$ and so $\lim_{k\to+\infty} \|A^k\mathbf{w}\| = 0$. It follows that the vector $A^k\mathbf{w}$ converges to the zero vector. ◊

Theorem 5.3 *If $\mathbf{v}_n \notin \mathcal{Z}_0$ for every n, then $\lim_{n\to+\infty} \|\mathbf{v}_n\| = 0$.*

PROOF: Result 6 implies that $\mathbf{v}_1 \notin \mathcal{Z}_{12}$. Let once again be $\beta = (1-k^2)/(1+k^2)$. By hypothesis, due to Result 6, we can take $k \in (0,1)$ and then $\beta \in (0,1)$.

Let us suppose that $\mathbf{v}_1 = (\dot\xi_1, \dot\eta_1) \in \mathcal{Z}_1$. Result 5 and the hypothesis imply that $\mathbf{v}_3 = (\dot\xi_3, \dot\eta_3) \in \mathcal{Z}_1$. Applying (14b,14c) we have

$$\begin{pmatrix} \dot\xi_3 \\ \dot\eta_3 \end{pmatrix} = \begin{pmatrix} -\varepsilon & -\beta\varepsilon(1+\varepsilon) \\ \beta(1+\varepsilon) & \beta^2(1+\varepsilon)^2 - \varepsilon \end{pmatrix} \begin{pmatrix} \dot\xi_1 \\ \dot\eta_1 \end{pmatrix}$$

Therefore, for every $h \in \mathbb{N}$, we have

$$\begin{pmatrix} \dot\xi_{2h+1} \\ \dot\eta_{2h+1} \end{pmatrix} = \begin{pmatrix} -\varepsilon & -\beta\varepsilon(1+\varepsilon) \\ \beta(1+\varepsilon) & \beta^2(1+\varepsilon)^2 - \varepsilon \end{pmatrix}^h \begin{pmatrix} \dot\xi_1 \\ \dot\eta_1 \end{pmatrix}$$

Moreover, if $\mathbf{v}_1 \in \mathcal{Z}_1$, by Result 5 and the hypothesis we have that $\mathbf{v}_2 \in \mathcal{Z}_2$. A straigthforward calculation shows that in this case, for every $h \in \mathbb{N}, h > 0$, we have

$$\begin{pmatrix} \dot\xi_{2h} \\ \dot\eta_{2h} \end{pmatrix} = \begin{pmatrix} \beta^2(1+\varepsilon)^2 - \varepsilon & \beta(1+\varepsilon) \\ -\beta\varepsilon(1+\varepsilon) & -\varepsilon \end{pmatrix}^h \begin{pmatrix} \dot\xi_2 \\ \dot\eta_2 \end{pmatrix} \tag{16}$$

Since the two matrices

$$H_1 = \begin{pmatrix} -\varepsilon & -\beta\varepsilon(1+\varepsilon) \\ \beta(1+\varepsilon) & \beta^2(1+\varepsilon)^2 - \varepsilon \end{pmatrix} \qquad H_2 = \begin{pmatrix} \beta^2(1+\varepsilon)^2 - \varepsilon & \beta(1+\varepsilon) \\ -\beta\varepsilon(1+\varepsilon) & -\varepsilon \end{pmatrix}$$

have the same characteristic polynomial and eigenvalues, then Theorem 5.2 and Remark 6 imply that $\lim_{n\to+\infty}(\dot\xi_n, \dot\eta_n) = (0,0)$ if the spectral radius $\rho(H_1) = \rho(H_2)$ is such that $\rho(H_1) < 1$. Therefore the theorem follows upon proof that $\rho(H_1) < 1$. Needless to say, the proof is completely analogous if $\mathbf{v}_1 \in \mathcal{Z}_2$.

If the eigenvalues λ_1, λ_2 of H_1 are complex conjugates or coincident, then $\rho(H_1) = |\lambda_1| = |\lambda_2| = \varepsilon < 1$. If the eigenvalues are both in $\mathbb{R}$ and distinct, they have the same sign and a standard study of

$$\rho(H_1)(\varepsilon,\beta) = \frac{1}{2}\left(\beta^2(1+\varepsilon)^2 - 2\varepsilon + \beta(1+\varepsilon)\sqrt{\beta^2(1+\varepsilon)^2 - 4\varepsilon}\right)$$

in the compact set $\overline{\Theta} = \left\{(\varepsilon,\beta) \middle| \varepsilon \in [0,1], \beta \in \left[\frac{2\sqrt{\varepsilon}}{1+\varepsilon}, 1\right]\right\}$ shows that, since $\dfrac{\partial\rho(H_1)}{\partial\beta} > 0$, the maximum is taken in the segment $\{\beta = 1\}$ and $\max_{\overline{\Theta}}(\rho(H_1)) = 1$. Then for every fixed $(\varepsilon,\beta) \in \Theta = \left\{(\varepsilon,\beta) \middle| \varepsilon \in (0,1), \beta \in \left(\frac{2\sqrt{\varepsilon}}{1+\varepsilon}, 1\right)\right\}$ we have $\max_{\Theta}(\rho(H_1)) < 1$, so that $\varepsilon \in (0,1), k \in (0,1)$ implies $\rho(H_1) \in [\varepsilon, 1)$. Since $\lim_{n\to+\infty} \|(\dot\xi_n, \dot\eta_n)\| = 0 = \lim_{n\to+\infty} \|(\dot x_n, \dot y_n)\|$ obviously implies that $\lim_{n\to+\infty} \|\mathbf{v}_n\|_2 = 0$, we have the thesis. □

REMARK 7. Let be $\mathbf{v}_0 \in \mathcal{Z}_{12}$ and $\varepsilon \in (0,1)$. A tedious but straightforward calculation[1] shows that

$$\|\mathbf{v}_1\|_2^2 - \|\mathbf{v}_0\|_2^2 = (\varepsilon^2 - 1)\,\frac{(k^2\dot x_0^2 + \dot y_0^2)^2}{k^4\dot x_0^2 + \dot y_0^2} < 0 \quad \Rightarrow \quad \|\mathbf{v}_1\|_2 < \|\mathbf{v}_0\|_2.$$

[1]The calculation was helped by the use of the factorization command of CoCoa©, a freely available program for computing with multivariate polynomials.

Moreover, another straightforward calculation shows that

$$\mathbf{v}_n \in \mathcal{Z}_1 \Rightarrow \|\mathbf{v}_{n+1}\|_2 < \|\mathbf{v}_n\|_2\,, \quad \mathbf{v}_n \in \mathcal{Z}_2 \Rightarrow \|\mathbf{v}_{n+1}\|_2 < \|\mathbf{v}_n\|_2 \quad \forall\, n \geq 0$$

and then the whole sequence $(\|\mathbf{v}_n\|_2)_{n\geq 0}$ decreases to 0. ◊

REMARK 8. Theorem 5.3 states a physical property of the mechanical system and not only a numerical property of TR_{nid}. For example, the same procedure of the proof applied starting from the rule (13) instead of (14) leads to the analysis of the spectral radius of the matrices

$$K_1 = \begin{pmatrix} \dfrac{(1-\varepsilon k^2)^2 - k^2(1+\varepsilon)^2}{(1+k^2)^2} & \dfrac{k(1-k^2)(1+\varepsilon)^2}{(1+k^2)^2} \\ -\dfrac{k(1-k^2)(1+\varepsilon)^2}{(1+k^2)^2} & \dfrac{(\varepsilon-k^2)^2 - k^2(1+\varepsilon)^2}{(1+k^2)^2} \end{pmatrix}$$

$$K_2 = \begin{pmatrix} \dfrac{(1-\varepsilon k^2)^2 - k^2(1+\varepsilon)^2}{(1+k^2)^2} & -\dfrac{k(1-k^2)(1+\varepsilon)^2}{(1+k^2)^2} \\ \dfrac{k(1-k^2)(1+\varepsilon)^2}{(1+k^2)^2} & \dfrac{(\varepsilon-k^2)^2 - k^2(1+\varepsilon)^2}{(1+k^2)^2} \end{pmatrix}.$$

It can be easily shown that the matrix B that expresses the change of coordinates (7) is such that $K_1 = B^{-1}H_1B, K_2 = B^{-1}H_2B$. The matrices H_1, H_2 and K_1, K_2 are then respectively similar, they have the same eigenvalues and then the same spectral radius. Similar arguments hold for every admissible change of coordinates. ◊

REMARK 9. For known results on matrices (the so called Gelfand's formula. See e.g. Theorem 4 in [Lax, 2002, p. 28]), the spectral radius $\rho(H_1)$ of the matrix H_1 can be expressed as a limit of matrix norms, that is

$$\rho(H_1) = \lim_{h\to\infty} \left\| H_1^h \right\|^{\frac{1}{h}}.$$

It follows that, for a large enough h, we have $\|H_1^h\| \approx \rho(H_1)^h$, and so

$$\|H_1^h v_1\| \leq \|H_1^h\|\|v_1\| \approx \rho(H_1)^h \|v_1\|. \tag{17}$$

Therefore the spectral radius $\rho(H_1) = \rho(K_1)$ gives also a measure of the rate of convergence to 0 of the velocity $\mathbf{v}_n$. It follows then from the proof of Theorem 5.3 that the bigger ε and β are, the slower the convergence is. This means that we can forecast slow convergence to 0 of the velocity for "almost elastic" walls and very small angles α. ◊

PART 2: NUMERICAL ASPECTS

6 Stable version of the algorithms

The theoretical rules TR can be easily implemented as described in this section, where we present an algorithm implementing the rule TR_{nid} for the non–ideal case, the ideal case being obtained by setting $\varepsilon = 1$.

For computational reasons, two thresholds $S \geq 0$ and $S_v \geq 0$ are introduced. If $S = S_v = 0$, the algorithm implements the theoretical rules TR_{nid}. Nevertheless, this choice of the thresholds presents some numerical drawbacks, because of the sensitivity of the algorithm to the noise on the input data and of its instability with respect to the floating point arithmetic: small perturbations of $\dot{\xi}_n$ and $\dot{\eta}$ can cause structural changes in response, e.g. it can happen that the exact $\dot{\xi}_n$ is a small negative value while the computed $\dot{\xi}_n$ is a small positive value, causing a different choice in the iterative method (see the example below). We choose a very small threshold $S > 0$ to consider as zero value the very small positive $\dot{\xi}_n$ or $\dot{\eta}_n$. Analogously, we choose a very small threshold $S_v > 0$ in order to consider as (almost) at rest a disk whose computed velocity is less than S_v. Moreover, in the while loop, we impose a maximum number of steps.

Algorithm implementing the rule TR_{nid}.

- **Input**: the coefficient $\varepsilon \in [0, 1]$, the angle $\alpha \in (0, \frac{\pi}{4}]$, the initial velocity $\mathbf{v}_0 = (\dot{x}_0, \dot{y}_0)$, with $\|\mathbf{v}_0\|_2 = 1$, the maximum number of steps N_{max} and two thresholds $S, S_v \geq 0$.
- **Output**: the final velocity $\mathbf{v}_f$.
- **First step**: $k = \tan(\alpha)$; $n = 0$; $\dot{\xi}_0 = k\dot{x}_0 + \dot{y}_0$; $\dot{\eta}_0 = k\dot{x}_0 - \dot{y}_0$.
- **Core**: While ($\dot{\xi}_n > S$ or $\dot{\eta}_n > S$), $n < N_{max}$, and $\|(\dot{x}_n, \dot{y}_n)\|_2 > S_v$:

  1. if ($\dot{\xi}_n \leq S$) and ($\dot{\eta}_n > S$), that is $(\dot{x}_n, \dot{y}_n) \in \mathcal{Z}_1$, then

$$\begin{cases} \dot{x}_{n+1} = \dfrac{1 - \varepsilon k^2}{1 + k^2}\dot{x}_n + \dfrac{(1+\varepsilon)k}{1 + k^2}\dot{y}_n \\ \dot{y}_{n+1} = \dfrac{(1+\varepsilon)k}{1 + k^2}\dot{x}_n - \dfrac{\varepsilon - k^2}{1 + k^2}\dot{y}_n \ ; \end{cases} \tag{18}$$

  2. if ($\dot{\xi}_n > S$) and ($\dot{\eta}_n \leq S$), that is $(\dot{x}_n, \dot{y}_n) \in \mathcal{Z}_2$, then

$$\begin{cases} \dot{x}_{n+1} = \dfrac{1 - \varepsilon k^2}{1 + k^2}\dot{x}_n - \dfrac{(1+\varepsilon)k}{1 + k^2}\dot{y}_n \\ \dot{y}_{n+1} = -\dfrac{(1+\varepsilon)k}{1 + k^2}\dot{x}_n - \dfrac{\varepsilon - k^2}{1 + k^2}\dot{y}_n \ ; \end{cases} \tag{19}$$

  3. if ($\dot{\xi}_n > S$) and ($\dot{\eta}_n > S$), that is $(\dot{x}_n, \dot{y}_n) \in \mathcal{Z}_{12}$, then

$$\begin{cases} \dot{x}_{n+1} &= \dfrac{-\varepsilon k^4 \dot{x}_n^2 + (1 - (1+\varepsilon)k^2)\dot{y}_n^2}{k^4\dot{x}_n^2 + \dot{y}_n^2}\dot{x}_n \\ \dot{y}_{n+1} &= \dfrac{k^2(k^2 - (1+\varepsilon))\dot{x}_n^2 - \varepsilon\dot{y}_n^2}{k^4\dot{x}_n^2 + \dot{y}_n^2}\dot{y}_n \ . \end{cases} \tag{20}$$

  4. $\dot{\xi}_{n+1} = k\dot{x}_{n+1} + \dot{y}_{n+1}$; $\dot{\eta}_{n+1} = k\dot{x}_{n+1} - \dot{y}_{n+1}$; $n = n + 1$.

- $\mathbf{v}_f = (\dot{x}_n, \dot{y}_n)$.

Later on, we denote with TA (Theoretical version of the Algorithm) the implementation with $S = S_v = 0$ and with SA (Stable version of the Algorithm) the implementation with $S, S_v > 0$.

The following example shows that TA is more sensible to the noise on the input data and to the floating point arithmetic computation than the SA, even in a very simple case.

EXAMPLE. We consider the behaviors of TA and SA when they process the initial velocity $\mathbf{v}_0 = (\dot{x}_0,\ \dot{y}_0) = (\frac{1}{\sqrt{2}},\ \frac{1}{\sqrt{2}})$, with $\alpha = \frac{\pi}{4}$ and $\varepsilon = 1$. From the theoretical point of view, TA and SA process the input data in the same way. Since $\mathbf{v}_0$ satisfies the condition of $\mathcal{Z}_2$, at the first iteration both algorithms compute the new velocity $\mathbf{v}_1 = (\dot{x}_1,\ \dot{y}_1) = (-\dot{y}_0,\ -\dot{x}_0) = (-\frac{1}{\sqrt{2}},\ -\frac{1}{\sqrt{2}})$. Since the coordinates of $\mathbf{v}_1$ satisfies the conditions in $\mathcal{Z}_0$ for both algorithms, TA and SA stop and $\mathbf{v}_1$ is the final computed velocity.

Nevertheless, when the algorithms are implemented, TA suffers from the data error and the computational approximation, while SA has the same behavior of the theoretical case, in the absence of errors. In fact, since the computed values of $\dot{x}_1$ and $\dot{y}_1$ are perturbed by errors, we obtain $\dot{x}_1 = -0.707106781186547$ and $\dot{y}_1 = -0.707106781186548$, so that $\dot{\xi}_1 = -0.707106781186547$ and $\dot{\eta}_1 = 4.440892098500626 \cdot 10^{-16}$. If $S = 0$, that is using an implementation of TA, $\dot{\xi}_1$ and $\dot{\eta}_1$ satisfy the conditions such that $\mathbf{v}_1 \in \mathcal{Z}_1$, and the algorithm compute a new iteration. Differently, choosing $S = 4.5 \cdot 10^{-16}$, that is twice the machine precision using a floating point arithmetic with $t = 52$ figures, SA is more robust: the values $\dot{\xi}_1$ and $\dot{\eta}_1$ satisfy the conditions such that $\mathbf{v}_1 \in \mathcal{Z}_0$, and the algorithm stops, as in the theoretical case. △

We saw that in the ideal case, TA determines a velocity such that the disk exits from the corner, while, in the non–ideal case, TA not always determines neither a velocity such that the disk exits from the corner nor a zero velocity, although the norm of the velocity decreases to 0 for increasing numbers of steps. For this reason the threshold N_{max} is introduced, in order to guarantee that the algorithm stops when the number of steps exceeds such a value. Analogously, the SA algorithm stops when both $\dot{\xi}_n$ and $\dot{\eta}_n$ are less than S, or when the 2-norm of the computed velocity is less than S_v, or when the number of steps exceeds N_{max}.

The computational complexity of an algorithm can be estimated by the amount of products required for computing the output. Since TA and SA are iterative algorithms, their computational complexity is given by the cost of each step times the number N of steps. Note that the coefficients involved in (18)–(20) can be computed once at the beginning of the algorithm, and so their cost can be neglected. Analogously, since the iteration (20) is computed at most only once, its cost can be neglected too. In conclusion, the final computational cost is $5N$, since (18) and (19) require 4 products and the tests on $\dot{\xi}$ and $\dot{\eta}$ require one additional product. For the ideal case, the value N can be computed using (9). For the non–ideal case, the maximum number of steps is the integer N such that $\|\mathbf{v}_N\| < S_v$. From (16) we have that $\|\mathbf{v}_{2n}\| \leq \|H_2^n\|\|v_0\| \approx \rho(H_2)^n\|\mathbf{v}_0\|$. Choosing $\|\mathbf{v_0}\| = \mathbf{1}$ and $S_v = 2^{-p}$, N can be estimated by $-2p/\log_2(\rho(H_2))$.
Finally, because of the low computational complexity of the algorithm, the execution time is so low as not to be significant: for the computational examples presented in [Fassino and Pasquero, 2019] the maximum execution time is less than $2 \cdot 10^{-3}$ seconds.

REMARK 10. Although the condition $k \in (0, \frac{\pi}{4}]$ entails the possibility of very small k, later on we suppose $k \gg S$. This is a very reasonable assumption for mechanical reasons, being $k = \tan\alpha$ a geometric quantity of a mechanical macroscopical system and the threshold S above of the same order of magnitude of the classical electron radius. ◊

7 Comparison between TA and SA

In the following we show that TA and SA compute the same final velocity in the same number of steps or, even if one of the algorithms executes more iterations, the final velocities are very similar. We can conclude that SA is preferable when we deal with real world measurements, since it produces analogous final velocities as TA, but it is more robust with respect to the errors on the input data.

Lemma 7.1 *Let $(\dot{x}_n, \dot{y}_n)$ be the linear velocity at the current step. Then:*

i) if $(\dot{x}_n, \dot{y}_n) \in \mathcal{Z}_1$ we have $|\dot{x}_{n+1} - \dot{x}_n| \leq \dot{\eta}_n$ *and* $|\dot{y}_{n+1} - \dot{y}_n| \leq 2\dot{\eta}_n$;

ii) if $(\dot{x}_n, \dot{y}_n) \in \mathcal{Z}_2$ we have $|\dot{x}_{n+1} - \dot{x}_n| \leq \dot{\xi}_n$ *and* $|\dot{y}_{n+1} - \dot{y}_n| \leq 2\dot{\xi}_n$.

PROOF: *i)* The thesis follows, since $\varepsilon, k < 1$, $\dot{\eta}_n > 0$ and since, by direct computation from (13b),

$$\dot{x}_{n+1} - \dot{x}_n = -\frac{(1+\varepsilon)k}{1+k^2}\dot{\eta}_n \quad \text{and} \quad \dot{y}_{n+1} - \dot{y}_n = \frac{(1+\varepsilon)}{1+k^2}\dot{\eta}_n \,.$$

Analogously for *ii)*, changing the role of $\dot{\xi}_n$ and $\dot{\eta}_n$. □

Lemma 7.2 *Let $\mathbf{v} = (\dot{x},\ \dot{y})$ and $\mathbf{v_p} = (\dot{x} + \delta_x, \dot{y} + \delta_y)$ be two velocity vectors such that both $\mathbf{v}$, $\mathbf{v_p} \in \mathcal{Z}_1$ or both $\mathbf{v}$, $\mathbf{v_p} \in \mathcal{Z}_2$. Let $\mathbf{w} = (\dot{t}, \dot{z})$ and $\mathbf{w_p} = (\dot{t}_p, \dot{z}_p)$ be the new computed velocity vectors starting from $\mathbf{v}$ and $\mathbf{v_p}$, respectively. Then*

i) $\left|\dot{t}_p - \dot{t}\right| \leq |\delta_x| + |\delta_y|$ *and* $|\dot{z}_p - \dot{z}| \leq |\delta_x| + |\delta_y|$;

ii) $\left|(k\dot{t}_p + \dot{z}_p) - (k\dot{t} + \dot{z})\right| \leq \frac{3}{2}|\delta_x| + |\delta_y|$ *and* $\left|(k\dot{t}_p - \dot{z}_p) - (k\dot{t} - \dot{z})\right| \leq \frac{3}{2}|\delta_x| + |\delta_y|$.

PROOF: If $\mathbf{v}, \mathbf{v_p} \in \mathcal{Z}_1$ then from (13b) we obtain

$$\dot{t}_p - \dot{t} = \frac{(1-\varepsilon k^2)}{1+k^2}\delta_x + \frac{(1+\varepsilon)k}{1+k^2}\delta_y \qquad \text{and} \qquad \dot{z}_p - \dot{z} = \frac{(1+\varepsilon)k}{1+k^2}\delta_x - \frac{\varepsilon - k^2}{1+k^2}\delta_y \,,$$

so that *i)* follows from $\varepsilon, k < 1$. Moreover, we have that

$$\begin{aligned}(k\dot{t}_p + \dot{z}_p) - (k\dot{t} + \dot{z}) &= \delta_x \frac{k(2 - \varepsilon k^2 + \varepsilon)}{1+k^2} + \delta_y \frac{2k^2 + \varepsilon k^2 - \varepsilon}{1+k^2} \quad \text{and} \\ (k\dot{t}_p - \dot{z}_p) - (k\dot{t} - \dot{z}) &= -k\varepsilon\delta_x + \varepsilon\delta_y \,.\end{aligned}$$

Since $\varepsilon, k \leq 1$, we have

$$0 \leq \frac{k(2 - \varepsilon k^2 + \varepsilon)}{1+k^2} \leq 3\frac{k}{1+k^2} \leq \frac{3}{2} \quad \text{and} \quad \left|\frac{2k^2 + \varepsilon k^2 - \varepsilon}{1+k^2}\right| = \left|1 - \frac{(1+\varepsilon)(1-k^2)}{1+k^2}\right| \leq 1 \,,$$

so that *ii)* follows. Analogous computation holds when $\mathbf{v}$, $\mathbf{v_p} \in \mathcal{Z}_2$. □

Proposition 7.1 *Starting from the same input, that is the same angle α, the same parameter ε and the same initial velocity vector $(\dot{x}_0,\ \dot{y}_0)$, TA and SA either compute the same output in the same number of steps, or they compute slightly different outputs, even if one of the algorithms performs more steps.*

	$\dot{\xi}_n \leq 0$	$0 < \dot{\xi}_n \leq S$	$\dot{\xi}_n > S$
$\dot{\eta}_n \leq 0$	TA and SA stop	TA: small changes SA stops	TA and SA in $\mathcal{Z}_2$
$0 < \dot{\eta}_n \leq S$	TA: small changes SA stops	TA: disk almost at rest SA stops	TA in $\mathcal{Z}_{12}$ SA in $\mathcal{Z}_2$
$\dot{\eta}_n > S$	TA and SA in $\mathcal{Z}_1$	TA in $\mathcal{Z}_{12}$ SA in $\mathcal{Z}_1$	TA and SA in $\mathcal{Z}_{12}$

Table 1: Behavior of TA and SA, starting from the same $(\dot{\xi}_n, \dot{\eta}_n)$.

PROOF: Let $(\dot{x}_n, \dot{y}_n)$ be the velocity vector, associated to $\dot{\xi}_n = k\dot{x}_n + \dot{y}_n$ and $\dot{\eta}_n = k\dot{x}_n - \dot{y}_n$, processed, at the n-th step, by both TA and SA. This is certainly verified at the first step, when $n = 0$.

First of all, we observe that, if $\|(\dot{x}_n, \dot{y}_n)\|_2 \leq S_v$, the disk is almost at rest and SA stops. Even if TA computes further iterations, since the 2-norm of the velocity is not increasing, its output is similar to the final velocity computed by SA.

If $\|(\dot{x}_n, \dot{y}_n)\|_2 > S_v$, we analyze the possible different cases, illustrated in Table 1.

In the following cases both TA and SA have the same behavior, that is they compute the same velocity vector $(\dot{x}_{n+1},\ \dot{y}_{n+1})$.

- If $\dot{\xi}_n \leq 0$ and $\dot{\eta}_n \leq 0$ both algorithms stop.
- If $\dot{\xi}_n \leq 0$ and $\dot{\eta}_n > S$, or $\dot{\xi}_n > S$ and $\dot{\eta}_n \leq 0$, or $\dot{\xi}_n > S$ and $\dot{\eta}_n > S$, both algorithms compute the same new velocity vector.

In the other cases, we show that TA and SA have different behaviors, but they compute similar outputs.

1. If $0 < \dot{\xi}_n \leq S$ and $0 < \dot{\eta}_n \leq S$, then SA stops and the disk can be considered almost at rest since $k \gg S$ and

$$\|(\dot{x}_n,\ \dot{y}_n)\|_2^2 = \frac{1+k^2}{4k^2}(\dot{\xi}_n^2 + \dot{\eta}_n^2) + \frac{1-k^2}{2k^2}\dot{\xi}_n\dot{\eta}_n \leq \frac{S^2}{k^2}\ .$$

   TA consider $(\dot{x}_n,\ \dot{y}_n) \in \mathcal{Z}_{12}$ and computes a new iteration. Since the 2-norm of the velocity vector decreases at each step also the output of TA corresponds to an almost at rest disk.

2. If $0 < \dot{\xi}_n \leq S$ and $\dot{\eta}_n \leq 0$, then SA stops, while TA computes a new velocity vector $(\dot{x}_{n+1},\ \dot{y}_{n+1})$ using (13c). From Lemma 7.1, $(\dot{x}_{n+1},\ \dot{y}_{n+1})$ differs from $(\dot{x}_n,\ \dot{y}_n)$, componentwise, for less than $2S$, since $0 < \dot{\xi}_n < S$. Moreover, $\dot{\xi}_{n+1} = -\varepsilon\dot{\xi}_n$, that is $-S < \dot{\xi}_{n+1} < 0$ and so, if $\dot{\eta}_{n+1}$ is negative, then TA stops and its output is similar to the one of SA. Otherwise, if $\dot{\eta}_{n+1}$ is positive, since $\dot{\eta}_n \leq 0$, we have

$$0 < \dot{\eta}_{n+1} = \dot{\eta}_n + (1+\varepsilon)\frac{1-k^2}{1+k^2}\dot{\xi}_n < (1+\varepsilon)\frac{1-k^2}{1+k^2}\dot{\xi}_n < 2S$$

   and so the disk is almost at rest, and we conclude, as in item 1, that TA and SA produce similar outputs. Analogously if $0 < \dot{\eta}_n \leq S$ and $\dot{\xi}_n \leq 0$.

3. If $0 < \dot{\xi}_n \leq S$ and $\dot{\eta}_n > S$, then SA and TA process the velocity vector $(\dot{x}_n,\ \dot{y}_n)$ in different ways. We have similar behaviors if $\dot{\xi}_n > S$ and $0 < \dot{\eta}_n \leq S$, changing the role of $\dot{\xi}_n$ and $\dot{\eta}_n$.

Let $0 < \dot\xi_n \le S$ and $\dot\eta_n > S$. SA computes $(\dot x^{(1)}_{n+1},\ \dot y^{(1)}_{n+1})$, $\dot\xi^{(1)}_{n+1} = k\dot x^{(1)}_{n+1} + \dot y^{(1)}_{n+1}$ and $\dot\eta^{(1)}_{n+1} = k\dot x^{(1)}_{n+1} - \dot y^{(1)}_{n+1}$, where

$$\begin{aligned} \dot x^{(1)}_{n+1} &= \frac{\dot\xi^{(1)}_{n+1} + \dot\eta^{(1)}_{n+1}}{2k} = \frac{1}{2k}\dot\xi_n + \frac{1-k^2-2\varepsilon k^2}{2k(1+k^2)}\dot\eta_n \qquad \text{and} \\ \dot y^{(1)}_{n+1} &= \frac{\dot\xi^{(1)}_{n+1} - \dot\eta^{(1)}_{n+1}}{2} = \frac{1}{2}\dot\xi_n + \frac{1-k^2+2\varepsilon}{2(1+k^2)}\dot\eta_n\ . \end{aligned}$$

Furthermore, $\dot\eta^{(1)}_{n+1} = -\varepsilon\dot\eta_n < 0$ and $0 < \dot\xi^{(1)}_{n+1} = \dot\xi_n + \frac{(1+\varepsilon)(1-k^2)}{1+k^2}\dot\eta_n < S + 2\dot\eta_n$.

TA computes $(\dot x^{(12)}_{n+1},\ \dot y^{(12)}_{n+1})$, $\dot\xi^{(12)}_{n+1} = k\dot x^{(12)}_{n+1} + \dot y^{(12)}_{n+1}$ and $\dot\eta^{(12)}_{n+1} = k\dot x^{(12)}_{n+1} - \dot y^{(12)}_{n+1}$, where

$$\dot x^{(12)}_{n+1} = \frac{\dot\xi^{(12)}_{n+1} + \dot\eta^{(12)}_{n+1}}{2k} = (\dot\xi_n + \dot\eta_n)\frac{(1-k^2-2\varepsilon k^2)(\dot\xi_n^2+\dot\eta_n^2) - 2(1-k^2)\dot\xi_n\dot\eta_n}{2kD}\ ,$$

$$\dot y^{(12)}_{n+1} = \frac{\dot\xi^{(12)}_{n+1} - \dot\eta^{(12)}_{n+1}}{2} = (\dot\eta_n - \dot\xi_n)\frac{(1-k^2+2\varepsilon)(\dot\xi_n^2+\dot\eta_n^2) + 2(1-k^2)\dot\xi_n\dot\eta_n}{2D}\ ,$$

where $D = (\dot\xi_n^2+\dot\eta_n^2)(1+k^2) + 2\dot\xi_n\dot\eta_n(k^2-1)$. Furthermore,

$$\dot\eta^{(12)}_{n+1} = \frac{-\varepsilon(\dot\xi_n^2+\dot\eta_n^2)(\dot\eta_n(1+k^2) - \dot\xi_n(1-k^2)) - \dot\xi_n(1-k^2)(\dot\xi_n^2+\dot\eta_n^2)}{D}$$

and, since $\dot\eta_n > \dot\xi_n$, then also $\dot\eta^{(12)}_{n+1} < 0$.

The velocities $(\dot x^{(1)}_{n+1}, \dot y^{(1)}_{n+1})$ and $(\dot x^{(12)}_{n+1}, \dot y^{(12)}_{n+1})$ are very similar, in fact

$$\begin{aligned} \dot x^{(1)}_{n+1} - \dot x^{(12)}_{n+1} &= \frac{\dot\xi_n k(1+\varepsilon)\left(\dot\eta_n^2(3-k^2) + \dot\xi_n^2(1+k^2)\right)}{D(1+k^2)} \\ \dot y^{(1)}_{n+1} - \dot y^{(12)}_{n+1} &= \frac{\dot\xi_n(1+\varepsilon)\left(\dot\eta_n^2(3k^2-1) + \dot\xi_n^2(1+k^2)\right)}{D(1+k^2)}\ . \end{aligned}$$

If we consider $\dot x^{(1)}_{n+1} - \dot x^{(12)}_{n+1}$ and $\dot y^{(1)}_{n+1} - \dot y^{(12)}_{n+1}$ as function of $\dot\xi_n$, using their Maclaurin series, we obtain

$$\dot x^{(1)}_{n+1} - \dot x^{(12)}_{n+1} = \frac{\dot\xi_n k(1+\varepsilon)(3-k^2)}{(1+k^2)^2} + O(\dot\xi_n^2) \quad \text{and} \quad \dot y^{(1)}_{n+1} - \dot y^{(12)}_{n+1} = \frac{\dot\xi_n(1+\varepsilon)(3k^2-1)}{(1+k^2)^2} + O(\dot\xi_n^2)\ .$$

Since $|\dot\xi_n| < S$, we can approximate such differences neglecting $O(\dot\xi_n^2)$:

$$\left|\dot x^{(1)}_{n+1} - \dot x^{(12)}_{n+1}\right| \approx \frac{\dot\xi_n k(1+\varepsilon)(3-k^2)}{(1+k^2)^2} < 2S \quad \text{and} \quad \left|\dot y^{(1)}_{n+1} - \dot y^{(12)}_{n+1}\right| \approx \frac{\dot\xi_n(1+\varepsilon)|3k^2-1|}{(1+k^2)^2} < 2S\ .$$

It follows that

$$\begin{aligned} \left|\dot\xi^{(1)}_{n+1} - \dot\xi^{(12)}_{n+1}\right| &< |k|\left|\dot x^{(1)}_{n+1} - \dot x^{(12)}_{n+1}\right| + \left|\dot y^{(1)}_{n+1} - \dot y^{(12)}_{n+1}\right| < 4S \\ \left|\dot\eta^{(1)}_{n+1} - \dot\eta^{(12)}_{n+1}\right| &< |k|\left|\dot x^{(1)}_{n+1} - \dot x^{(12)}_{n+1}\right| + \left|\dot y^{(1)}_{n+1} - \dot y^{(12)}_{n+1}\right| < 4S\ . \end{aligned}$$

Summing up, we have

$$\dot\xi^{(1)}_{n+1} > 0\ , \qquad \dot\eta^{(1)}_{n+1} < 0\ , \qquad \dot\xi^{(1)}_{n+1} - 4S < \dot\xi^{(12)}_{n+1} < \dot\xi^{(1)}_{n+1} + 4S\ , \qquad \dot\eta^{(1)}_{n+1} - 4S < \dot\eta^{(12)}_{n+1} < 0\ .$$

Since $\dot\eta^{(1)}_{n+1}, \dot\eta^{(12)}_{n+1} < 0$, if one of TA and SA does not stop, then it computes a new velocity vector using the formulae of $\mathcal{Z}_2$.

In general, there are the following cases.

a) $0 < \dot{\xi}^{(1)}_{n+1} \leq S$ and $\dot{\xi}^{(12)}_{n+1} \leq 0$. Since $\dot{\eta}^{(1)}_{n+1} < 0$ and $\dot{\eta}^{(12)}_{n+1} < 0$, SA and TA stop and return the similar outputs $(\dot{x}^{(1)}_{n+1},\ \dot{y}^{(1)}_{n+1})$ and $(\dot{x}^{(12)}_{n+1},\ \dot{y}^{(12)}_{n+1})$.

b) $0 < \dot{\xi}^{(1)}_{n+1} \leq S$ and $\dot{\xi}^{(12)}_{n+1} > 0$. Since $\dot{\eta}^{(1)}_{n+1} < 0$, SA stops.
Since $\dot{\eta}^{(12)}_{n+1} < 0$, TA uses the formulae in $\mathcal{Z}_2$. We have $0 < \dot{\xi}^{(12)}_{n+1} \leq \dot{\xi}^{(1)}_{n+1} + 4S < 5S$ and $\eta^{(12)}_{n+1} < 0$, and so Lemma 7.1 implies that TA performs small changes to $(\dot{x}^{(12)}_{n+1}, \dot{y}^{(12)}_{n+1})$. Moreover, $\dot{\xi}_{n+2} = -\varepsilon\dot{\xi}^{(12)}_{n+1}$ and so $-5S < \dot{\xi}_{n+2} < 0$. If $\dot{\eta}_{n+2} \leq 0$, then TA stops with a similar output as SA. Otherwise, if $\dot{\eta}_{n+2} > 0$, then, since $\dot{\eta}^{(12)}_{n+1} < 0$,

$$0 < \dot{\eta}_{n+2} = \dot{\eta}^{(12)}_{n+1} + (1+\varepsilon)\frac{1-k^2}{1+k^2}\dot{\xi}^{(12)}_{n+1} < (1+\varepsilon)\frac{1-k^2}{1+k^2}\dot{\xi}^{(12)}_{n+1} < 10S\ .$$

In this case, since $\dot{\xi}^{(12)}_{n+1}$ and $\dot{\eta}^{(12)}_{n+1}$ are very small, the disk, at the $(n+1)$-th step, is almost at rest and the outputs of TA and SA are very similar, independently of the number of steps performed by TA, after SA has stopped.

c) $\dot{\xi}^{(1)}_{n+1} > S$ and $\dot{\xi}^{(12)}_{n+1} \leq 0$. Since $\eta^{(12)}_{n+1} < 0$, TA stops.
Since $\dot{\eta}^{(1)}_{n+1} < 0$, SA uses the formulae in $\mathcal{Z}_2$. Since $0 > \xi^{(12)}_{n+1} > \xi^{(1)}_{n+1} - 4S$, then $S < \xi^{(1)}_{n+1} < 4S$ and, from Lemma 7.1, SA performs small changes to $(\dot{x}^{(1)}_{n+1}, \dot{y}^{(1)}_{n+1})$. Since $\dot{\xi}_{n+2} = -\varepsilon\dot{\xi}^{(1)}_{n+1}$, we have $-4S < \dot{\xi}_{n+2} < 0$ and, if $\dot{\eta}_{n+2} \leq S$, then SA stops and it returns a final velocity similar to the output of TA. Otherwise, if $\dot{\eta}_{n+2} > S$, since $\dot{\eta}^{(1)}_{n+1} < 0$, we have that

$$S < \dot{\eta}_{n+2} = \dot{\eta}^{(1)}_{n+1} + (1+\varepsilon)\frac{1-k^2}{1+k^2}\dot{\xi}^{(1)}_{n+1} < (1+\varepsilon)\frac{1-k^2}{1+k^2}\dot{\xi}^{(1)}_{n+1} < 8S\ .$$

In this case, since $\dot{\xi}^{(12)}_{n+1}$ and $\dot{\eta}^{(12)}_{n+1}$ are very small, the disk, at the $(n+1)$-th step, is almost at rest and the output of TA and SA is very similar, independently of the number of steps performed by SA, after TA has stopped.

d) $\dot{\xi}^{(1)}_{n+1} > S$ and $\dot{\xi}^{(12)}_{n+1} > 0$. Both TA and SA compute, using the same formulae in $\mathcal{Z}_2$, a new iteration starting from two similar velocities. Lemma 7.2 implies that the new computed velocities slightly differ from each other. Moreover, the new values of $\dot{\xi}$, equal to $-\varepsilon\dot{\xi}^{(1)}_{n+1}$ and $-\varepsilon\dot{\xi}^{(12)}_{n+1}$ respectively, are negative, so that we can repeat an analysis of the behavior of TA and SA analogous to the one presented in items a – d, changing the role of $\dot{\xi}$ and $\dot{\eta}$.

In conclusion, SA and TA compute similar final velocities, even if they can perform a different number of iterations. In fact the following cases happen.

- Both algorithms have the same behavior, that is they compute the same iterations.
- SA and TA stops at the same iterations and return similar final velocities.
- SA and TA perform a different number of iterations. Two different cases can happen. Either one of the algorithms performs only one iteration more than the other, making small changes to the new computed velocity or the disk is almost at rest, so that both final velocities are similar even if one algorithm performs some more iterations.

□

8 Numerical Examples

In the following we show in a compact visualization the results of the stable algorithm performed in some significant cases. In each figure, we represent input and outputs of the impact of a unitary disk with the walls. In each figure, the walls forming the angle 2α are visualized with two segments tangent to the disk in the contact points and the unitary initial velocity $\mathbf{v}_0 = (\cos\varphi_0, \sin\varphi_0)$ is visualized with a dashed line ending with an empty dot on the border of the disk. In each figure, the outputs are visualized for different values of the restitution coefficient ε: a full dot visualizes direction and norm of output velocities belonging to $\mathcal{Z}_0$, no marks visualize output velocities having an "almost at rest condition" norm. The figures show the results for $\varepsilon \in \{1, 0.75, 0.5, 0.25, 0.05\}$ in the following cases (a wider set of results of the stable algorithm, presented in tabular form and briefly analyzed, can be found in [Fassino and Pasquero, 2019]):

a$_1$) $\alpha = \dfrac{\pi}{6}$, $\tan\varphi_0 = \dfrac{k}{2} = \dfrac{\tan\alpha}{2}$ (see Fig.a_1);

a$_2$) $\alpha = \dfrac{\pi}{6}$, $\tan\varphi_0 = k = \tan\alpha$, ($\mathbf{v}_0 \in \mathcal{Z}_2$ and parallel to a wall. Fig.a_2);

b$_1$) $\alpha = \dfrac{\pi}{16}$, $\tan\varphi_0 = \dfrac{k}{2} = \dfrac{\tan\alpha}{2}$ (see Fig.b_1);

b$_2$) $\alpha = \dfrac{\pi}{16}$, $\tan\varphi_0 = k = \tan\alpha$, ($\mathbf{v}_0 \in \mathcal{Z}_2$ and parallel to a wall. Fig.b_2);

c$_1$) $\alpha = \dfrac{\pi}{32}$, $\tan\varphi_0 = \dfrac{k}{2} = \dfrac{\tan\alpha}{2}$ (see Fig.c_1);

c$_2$) $\alpha = \dfrac{\pi}{32}$, $\tan\varphi_0 = k = \tan\alpha$, ($\mathbf{v}_0 \in \mathcal{Z}_2$ and parallel to a wall. Fig.c_2).

The figures show a satisfactory agreement between numerical and theoretical results, with a meaningful physical interpretation. With the predictable exception of the ideal case, the narrowing of the angle between the walls and the decreasing of the restitution coefficient reduce the possibility of an effective exit of the disk from the corner and, even in this case, reduce the norm of the exit velocity. Vice versa, they increase the possibility of achieving a "rest" condition for the disk in the corner.

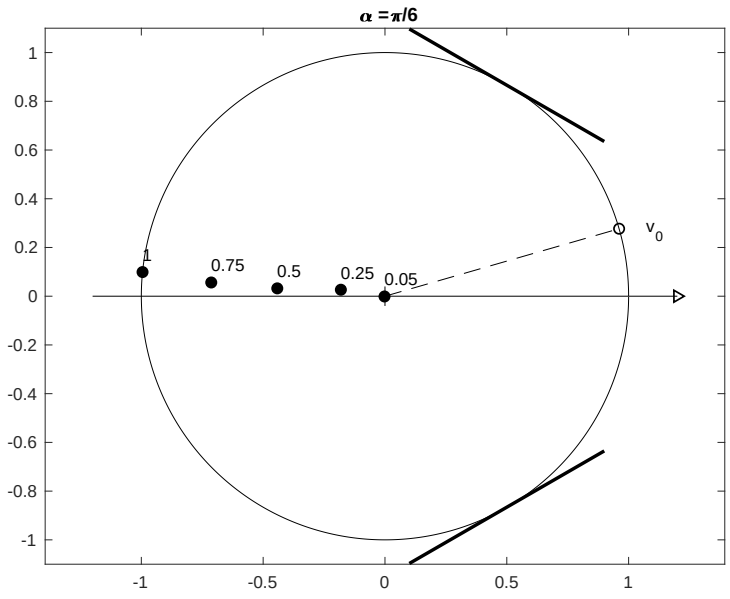

Figure a_1

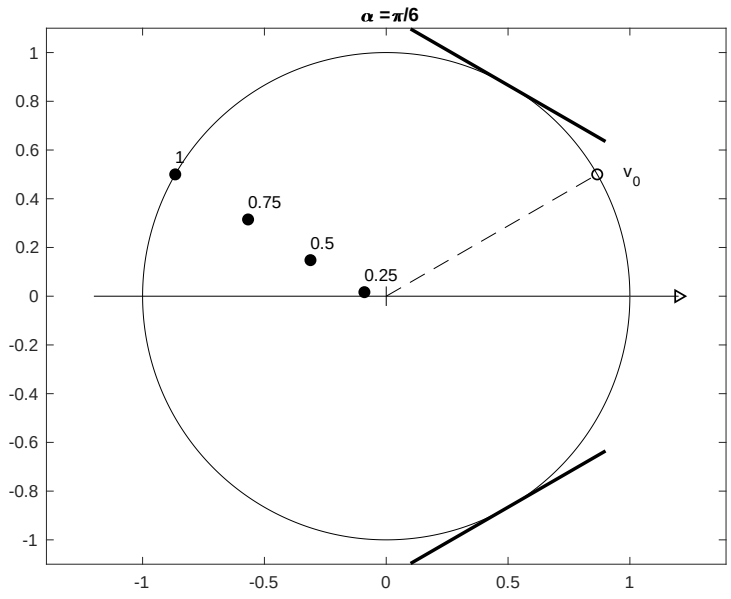

Figure a_2

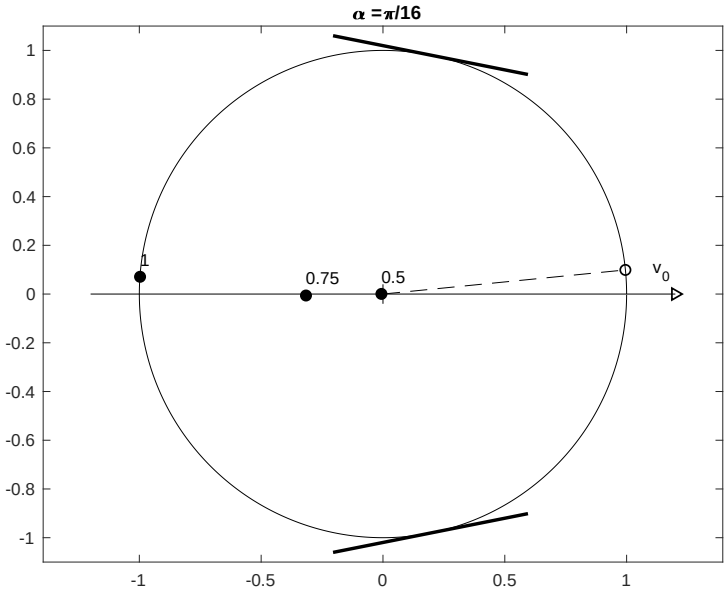

Figure b_1

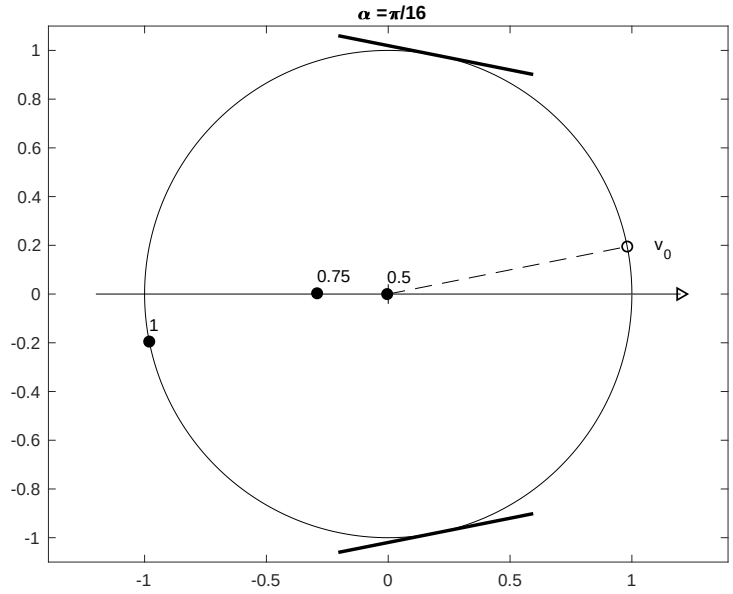

Figure b_2

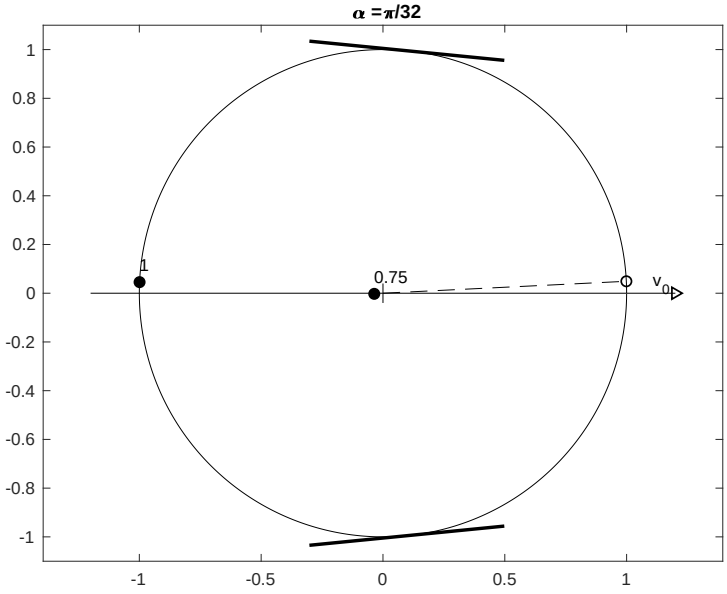

Figure c_1

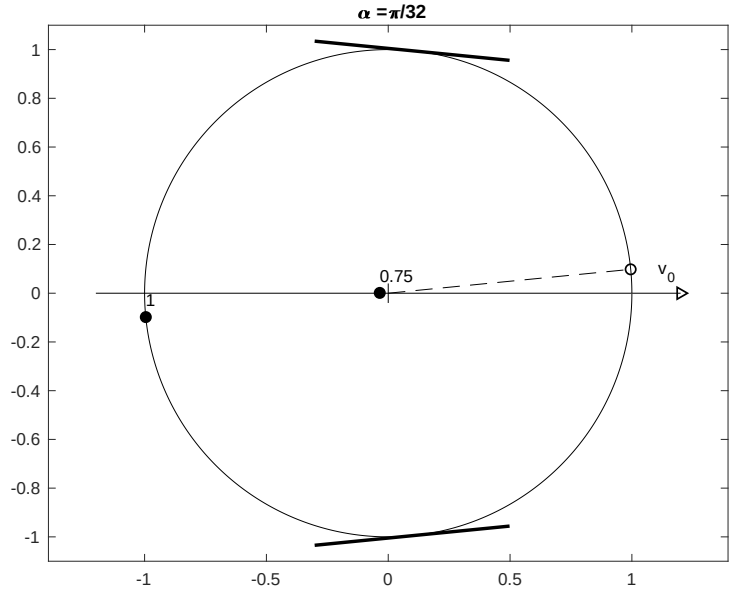

Figure c_2

9 Conclusions

We showed that the theoretical iterative procedure described in ([Pasquero, 2018]) for determining the exit velocity of a mechanical system having a multiple impact can be effectively applied to the the study of the behavior of the basic planar system given by a disk impacting without friction with the walls of a corner, and the applicability can be extended to non–ideal cases without the preservation of the kinetic energy required in ([Pasquero, 2018]). The simpleness of the system allows:

- to proof several theoretical results (termination of the iterative procedure in a finite number of steps in the ideal case, norm of the velocity decreasing, possibly to zero, in the non–ideal case) in good agreement with meaningful physical interpretations;
- an effective implementation of the procedure through a stable algorithm that:
  - gives a meaningful output (the 2–dimensional exit velocity) starting from a small set of input data (the 2–dimensional entrance velocity, the angle of the corner, the restitution coefficient of the walls of the corner);
  - requires a very low computational time, e.g. for the computational examples presented in [Fassino and Pasquero, 2019] the maximum execution time is less than $2 \cdot 10^{-3}$ seconds;
  - is robust, so that small perturbation of the input data and approximations of computed values does not invalidate or significantly change the output and their physical meaning.
- straightforward generalizations to rigid bodies different from the disk, such as rocking blocks ([Yilmaz et al., 2009]).

However, the limits of the method are the limits of its theoretical approach:

– the impact and its effects are supposed instantaneous, no time integrations are performed and no information on the motion of the disk in a finite time interval are obtained. For this reason, the method affects the complexity of a time–integration procedure only in the determination of new initial data for the time integration;

– the possible presence of friction and/or compliance are not taken into account.

References

[Acary and Brogliato, 2008] Acary, V. and Brogliato, B. (2008). *Numerical Methods for Nonsmooth Dynamical Systems: Applications in Mechanics and Electronics.*, volume 35. Springer Verlag.

[Brogliato, 2016] Brogliato, B. (2016). *Nonsmooth Impact Mechanics. Models, Dynamics and Control - Third Edition.* Springer International Publishing Switzerland; Communications and Control Engineering.

[Fassino and Pasquero, 2019] Fassino, C. and Pasquero, S. (2019). An algorithmic approach to the multiple impact of a disk in a corner. *arXiv:1902.05147*.

[Haddouni et al., 2017] Haddouni, M., Acary, V., Garreau, S., Beley, J., and Brogliato, B. (2017). Comparison of several formulations and integration methods for the resolution of daes formulations in event-driven simulation of nonsmooth frictionless multibody dynamics. *Multibody System Dynamics*, 41(3):201–231.

[Isaacson and Keller, 1994] Isaacson, E. and Keller, H. (1994). *Analysis of Numerical Methods.* Dover, New York.

[Johnson, 1985] Johnson, K. (1985). *Contact mechanics.* Cambridge University Press, Cambridge.

[Khulief, 2013] Khulief, Y. (2013). Modeling of impact in multibody systems: An overview. *ASME J. Comp. Nonlin. Dyn.*, 8.

[Kiseleva et al., 2018] Kiseleva, M., Kuznetsov, N., and Leonov, G. (2018). Theory of differential inclusions and its application in mechanics. *New Perspectives and Applications of Modern Control Theory: In Honor of Alexander S. Poznyak*, pages 219–239.

[Lax, 2002] Lax, P. D. (2002). *Functional Analysis*. Wiley-Interscience.

[Liu et al., 2008] Liu, C., Zhao, Z., and Brogliato, B. (2008). Frictionless multiple impacts in multibody systems. i. theoretical framework. In *Proceedings of the Royal Society of London A: Mathematical, Physical and Engineering Sciences*, volume 464, pages 3193–3211. The Royal Society.

[Lötstedt, 1982] Lötstedt, P. (1982). Mechanical systems of rigid bodies subject to unilateral constraints. *SIAM Journal on Applied Mathematics*, 42(2):281–296.

[Monteiro Marques, 1993] Monteiro Marques, M. (1993). *Differential Inclusions in Non-smooth Mechanical Problems: Shocks and Dry Friction.* Birkhuser, Boston.

[Moreau, 1988] Moreau, J. (1988). Unilateral contact and dry friction in finite freedom dynamics. In *Nonsmooth Mechanics And Applications*, pages 1–83. Springer Verlag, Wien – New York.

[Moreau, 1999] Moreau, J. (1999). Numerical aspects of the sweep-ing process. *Computer Methods in Applied Mechanicsand Engineering*, 177:329349.

[Negrut et al., 2007] Negrut, D., Rampalli, R., Ottarson, G., and Sajdak, A. (2007). On an implementation of the hht method in the context of index 3 differential algebraic equations of multibody dynamics. *ASME J. Comp. Nonlin. Dyn.*, 2:73–85.

[Paoli and Schatzman, 2002] Paoli, L. and Schatzman, M. (2002). A numerical scheme for impact problems i: The one-dimensional case. *SIAM Journal of Numerical Analysis*, 40(2):702–733.

[Pasquero, 2005] Pasquero, S. (2005). Ideality criterion for unilateral constraints in time–dependent impulsive mechanics. *Journ. Math. Phys.*, 46,n.11:112904–20pp.

[Pasquero, 2018] Pasquero, S. (2018). Ideal characterizations of multiple impacts: A frame–independent approach by means of jet–bundle geometry. *Quarterly of Applied Mathematics*, 76(3):547–576.

[Pfeiffer and Glocker, 2000] Pfeiffer, F. and Glocker, C. (2000). *Multibody dynamics with unilateral contacts*, volume 421. Springer Science & Business Media.

[Stronge, 2000] Stronge, W. (2000). *Impact Mechanics*. Cambridge University Press., Cambridge.

[Yilmaz et al., 2009] Yilmaz, C., Gharib, M., and Hurmuzlu, Y. (2009). Solving frictionless rocking block problem with multiple impacts. *Proc. R. Soc. A Proc. R. Soc. A*, 465:3323–3339.